AN AUTOMATIC-THROTTLE DEVICE FOR AIRSPEED CONTROL DURING FLARE TO FIELD LANDINGS

ROBERT L. ELICH

AN AUTOMATIC-THROTTLE DEVICE FOR AIRSPEED CONTROL DURING FLARE TO FIELD LANDINGS

by

Robert Louis Elich
Lieutenant Commander, United States Navy
B.S., University of Colorado, 1957

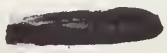

Submitted in partial fulfillment
for the degree of

MASTER OF SCIENCE IN AERONAUTICAL ENGINEERING

from the

UNITED STATES NAVAL POSTGRADUATE SCHOOL
May 1966

ABSTRACT

This study is a continuation of the investigations in the use of automatic-throttle compensation systems. The previous investigations demonstrated the capability of such systems in alleviating the problems of aircraft speed instability in the carrier landing approach. The feasibility of adapting the system with sensed-input variables of angle-of-attack and normal acceleration to the condition of field landings with flare was investigated. An analysis of the ground effect prevalent in field landings was performed and the significant influences on aircraft response were included in the investigation. The desired airspeed control with zero rate of descent at touchdown was obtained by incorporating additional commands in the basic auto-throttle device during the flare maneuver. The analog computer was utilized for problem simulation.

This investigation was performed by LCDR Robert L. Elich, USN, at the U. S. Naval Postgraduate School, Monterey, California.

TABLE OF CONTENTS

LIST OF TABLES

LIST OF ILLUSTRATIONS

LIST OF SYMBOLS

General

A	Aspect ratio
B	Moment of inertia about the Y axis
b	Wing span
C_D	Drag force coefficient
C_L	Lift force coefficient
C_m	Pitching moment coefficient
$\bar{c}$	Mean geometric chord
g	Gravitational acceleration
H	Height above ground
h	Center of gravity position, fraction of mean chord
$h_{n_{w_b}}$	Neutral point of the wing-body combination
K	Constant
l_t	Distance between center of gravity and tail aerodynamic center
M	Pitching moment
m	Aircraft mass
n'	Acceleration force in "g" units
n	Increment of Acceleration force in "g" units
q	Angular velocity in pitch
S	Reference area
T	Thrust
U	Velocity parallel to X body axis

u	Velocity perturbation parallel to X body axis
V	Relative velocity
W	Aircraft weight
w	Velocity perturbation parallel to Z body axis
X	Force acting parallel to X body axis
Z	Force acting parallel to Z body axis

Greek Symbols

α	Angle-of-attack
γ	Glide slope angle
Γ	Circulation
ϵ	Downwash angle
η	Elevator deflection angle
Θ	Pitch attitude, steady state
θ	Pitch attitude perturbation
τ	Time constants

Subscripts

b	Body
G	In ground effect
l	Two dimensional lift
o	Initial or steady state condition
T	Horizontal tail
w	Wing

Derivatives

C_{D_α} Partial of C_D with respect to α

C_{D_u} Partial of C_D with respect to u

C_{L_α} Partial of C_L with respect to α

$C_{L_{\alpha_T}}$ Partial of C_L with respect to α of tail

$C_{L_{\alpha_{wb}}}$ Partial of C_L with respect to α_{wb}

C_{m_α} Partial of C_m with respect to α

C_{m_η} Partial of C_m with respect to η

C_{m_q} Partial of C_m with respect to pitch rate, q

1. Introduction.

This study is a continuation of the investigations being conducted at the U. S. Naval Postgraduate School on automatic-throttle compensation systems. The previous studies conducted by Lieutenant Commander G. R. Bell [1], and Lieutenant R. E. Evans and Captain R. H. Schuppe [2] were presented in 1963 and 1964 respectively.

As shown in Ref. 1 and Ref. 2 automatic-throttle compensation system utilizing various sensed-input variables are capable of alleviating the speed instability difficulties of modern supersonic aircraft during carrier landing approaches. One such system utilizes angle-of-attack change and change in acceleration normal to glide slope for commands to initiate the proper change in engine thrust. The purpose of this investigation was to determine the feasibility of adapting this system to the condition of normal field landing which is terminated with a flare maneuver to the touchdown. It is proposed that by incorporating additional commands to the basic auto-throttle system during the flare maneuver, a decrease in airspeed to a desired minimum at touchdown can be accomplished simultaneously with zero rate-of-descent.

The linearized, full equations of motion derived from small perturbation theory were used for this analysis. The coefficients in the equations were assumed constant except for those directly affected by the aircraft flying in close proximity to the ground. The influence of ground effect on the dynamic stability due to the varying coefficients was investigated and

was included in this study.

The vehicle used in this and the previous studies is the Navy swept wing fighter, F-8. The Donner 3100 Analog Computer with associated equipment was utilized to simulate the aircraft motion and maneuvering response with the proposed auto-throttle device.

2. Basic Automatic-throttle (α - n) System.

The type of automatic-throttle controller presently used in the Navy F-8 is Specialties, Inc. Automatic-Power Compensator, (APC), which utilizes sensed-input variables of angle-of-attack, α, and normal acceleration, n, for engine thrust command. A block diagram, typical of this system is shown in Figure 1. For the design application of this system, constant glide slope and airspeed are desired throughout the approach and the two sensed variables of instantenous angle-of-attack and acceleration normal to the glide slope in "g" units are the engine command functions. The use of these variables as the command functions for airspeed control is evident from the relationship:

$$L = n'w = \frac{1}{2}\rho V^2 S C_L$$

$$n'W = \frac{1}{2}\rho V^2 S C_{L_\alpha} \alpha$$

$$\frac{n'}{\alpha} = \frac{1}{2}\rho V^2 \frac{S}{W} C_{L_\alpha}$$

$$\frac{n'}{\alpha} = \text{Const.}\ (V^2)$$

From this equality, and increase of velocity results from a positive normal

acceleration increment and a velocity decrease results from a positive angle-of-attack increment. Thus, the normal acceleration in "g" units and angle-of-attack are inputs which are converted into the thrust command by the system computer utilizing chosen gain and time factors. The resulting change of thrust from the engine acts as a forcing function to the airframe modes of motion appropriately changing the aircraft velocity. The APC computer indirectly controls the aircraft velocity through the equations:

$$\Delta T = K_{\alpha}\Delta\alpha + K_{n}\Delta n'$$

since $\Delta V = K_{T}\Delta T$

therefore, $\Delta V = K'_{\alpha}\Delta\alpha + K'_{n}\Delta n'$

where the K values are the appropriate shaping, filtering and simulation networks.

The transfer function for the thrust command as specified by Specialties, Inc. is:

$$\Delta T_{c} = \frac{1}{(1+\tau_{e}S)} \frac{1}{(1+\tau_{s}S)} \left[\left(\frac{K_{\alpha}}{1+\tau_{\alpha}S} + \frac{K_{\gamma}}{S} + \frac{K_{1}}{1+S} \right) \alpha - \frac{Kn}{1+\tau_{n}S} n \right]$$

where,

τ_{s} - 0.2 sec (throttle servo time constant)

τ_{α} - 0.5 sec (angle of attack filter time constant)

τ_{e} - 1.2 sec (engine time lag)

τ_{n} - 1.0 sec (normal acceleration filter time constant)

K_{α} - 570 lb/deg. (angle-of-attack displacement gain)

K_{γ} - 190 lb/deg-sec (angle-of-attack intergral gain)

K_1' - 1,100 lb/deg (angle-of-attack gain)

K_n - 19,400 lb/"g" (normal acceleration gain)

As evidenced from the transfer function, the effect of increasing the instantaneous angle-of-attack results in an opening of the throttle and an increase of thrust, and a decrease in thrust is obtained for a decrease in angle-of-attack. An increment of normal acceleration is seen as a negative element in the transfer function with the effect of decreasing the thrust for a postive "g" perturbation and increasing the thrust for a negative "g" perturbation. Ref. 1, 2, and 3 support the validity of this auto-throttle device for use in carrier landing approaches.

3. Discussion of Auto-throttle System in Field Landings.

In the field landing phase, it is desired that just prior to touchdown the vertical kinetic energy be dissipated and the horizontal kinetic energy be a minimum contingent on the minimum safe airspeed. Thus, structural damage and wear and tear on aircraft components will be minimized along with the advantage of using shorter runways. From the pilots point of view, these results are attained by application of elevator to flare the aircraft as necessary to decelerate to the desired touchdown airspeed with zero rate-of-descent.

It is proposed that the α - n auto-throttle system can be utilized to accomplish the desired airspeed control by incorporating a supplementary circuit in the designed APC. For the purpose of this investigation, it was

assumed that the F-8 aircraft was making an Instrument Landing System (ILS) approach with a four degree glide slope on the recommended approach speed of 1.2 V_{SL} = 139 Kt. commencing a flare at 100 ft. above the ground, approximately eight seconds prior to touchdown. The desired airspeed for touchdown was 1.05 V_{SL} = 123 Kt. or 209 ft/sec.

Since it is mandatory that the auto-throttle system be unchanged up to the flare maneuver, it was decided that the proposed supplementary circuit of the APC be separately energized at this point. This circuit would supply the auto-throttle device with additional angle-of-attack and/or normal acceleration signals changing the error signals received. Thus, in effect a new base for the auto-throttle system is created. The error signal changes shall be referred to as "biasing" throughout the remainder of this study.

The method of applying the angle-of-attack bias was determined from the equation describing the change in pitching moment coefficient from straight to rotational flight:

$$\Delta C_m = C_{m_\alpha} \Delta\alpha + C_{m_\eta} \Delta\eta + C_{m_q} q$$

Assuming that the change in moment is zero and neglecting the change in moment due to rate of pitch, q, the resulting equation is:

$$C_{m_\alpha} \Delta\alpha \approx - C_{m_\eta} \Delta\eta$$

$$\Delta\alpha \approx - \frac{C_{m_\eta}}{C_{m_\alpha}} \Delta\eta$$

$$\Delta\alpha \approx \text{Const.} \; (\Delta\eta)$$

Thus, the angle-of-attack bias was experimentally utilized as some percent-

age of $\Delta\eta$.

Since it has been previously determined that the average pilot pulls a maximum of + 0.2 g above the 1 g steady state condition during the flare maneuver [4], the normal acceleration bias was experimentally utilized as a percentage of 0.2 g.

4. Equations of Motion.

The basic three degree of freedom longitudinal equations of motion based on body axes used for this analysis are shown below. These equations were derived from linearized theory based on small disturbances from a reference steady state flight condition. Full derivation and definitions are included as Appendix I. The equations are shown in the dimensional form necessary for analog simulation.

X FORCE:

$$\dot{u} - \frac{X_u}{m} u - \frac{X_\alpha}{m} \alpha + g \cos \Theta \theta = \frac{X_{\Delta T}}{m} \Delta T$$

Z FORCE:

$$- \frac{Z_u}{mU_o} u + \dot{\alpha} - \frac{Z_w}{m} - \theta = \frac{Z_\eta}{mU_o} \eta$$

MOMENT EQUATION:

$$- \frac{M_u}{B} u - \frac{M_{\dot{\alpha}}}{B} \dot{\alpha} - \frac{M_\alpha}{B} \alpha + \ddot{\theta} - \frac{M_q}{B} \dot{\theta} = \frac{M_{\Delta T}}{B} \Delta T + \frac{M_\eta}{B} \eta$$

The values of the dimensional stability derivatives and aircraft parameters as obtained from Ref. 3 are included as Table I and Table II respectively.

5. Ground Effect.

The principal effects of the ground on a nearby aircraft are increases

of the slope of the lift curves of the wing and tail and a decrease in the downwash at the tail. These changes result from the constraint of the vortex patterns at and behind the wing. The effects may be approximated by superimposing an image vortex system, as shown below, beneath the ground having induced velocities of necessary magnitude to satisfy the boundary condition of no flow across the ground plane[1]. This method of approximation utilizes only the trailing vortices as it is normally considered that the bound vortex patterns cancel each other. The trailing image vortex will decrease the downwash at the tail and decrease the downwash in the tail and wing planes which increases the slopes of the lift curves.

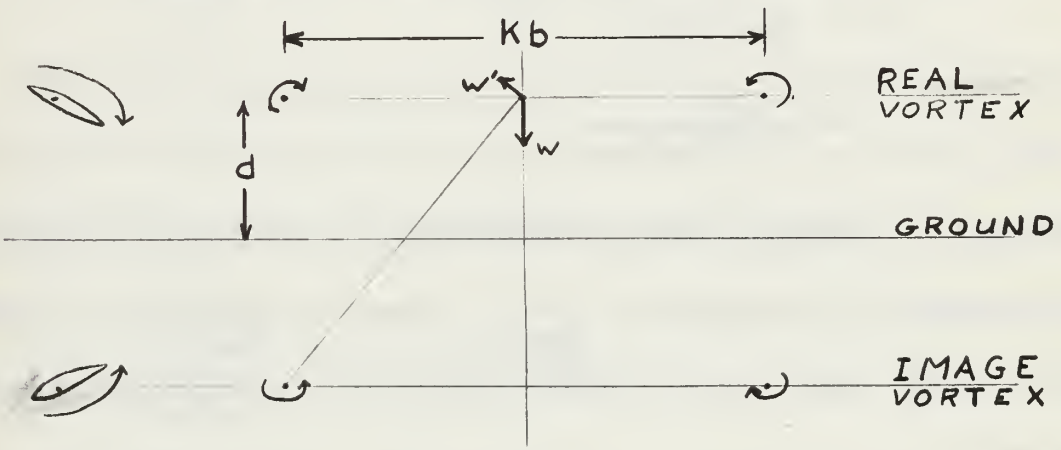

For a two dimensional lifting surface, the Kutta-Joukowski theorem states that the lift is equal to the density times velocity times circulation or

$$L = \rho V \Gamma \quad \text{lb/ft. of span}$$

[1]Andrews, E. J., Notes on Simplified Ground Effect Analysis. U. S. Naval Postgraduate School, Monterey, California

Thus the local lift coefficient is:

$$C_l = \frac{\rho V \Gamma}{\frac{1}{2}\rho V^2 c}$$

$$= \frac{2\Gamma}{c V}$$

For an airfoil with uniform span loading with the associated trailing vortices a distance Kb apart, where b is the span, the induced velocity at the aircraft centerline is:

$$w = 2\frac{\Gamma}{4\pi Kb/2}$$

Since the downwash, ϵ, is defined as $\frac{w}{V}$, then

$$\epsilon = \frac{\Gamma}{2\pi V Kb/2}$$

$$= \frac{C_l c}{4\pi Kb/2}$$

Therefore, the change in downwash with respect to the change in the local lift coefficient is proportional to $\frac{1}{Kb/2}$. Resolving the induced velocities from the image vortex system into the vertical plane at the aircraft centerline results in:

$$w' = \frac{2\Gamma}{4\pi\left[\left(\frac{Kb}{2}\right)^2 + (2d)^2\right]^{\frac{1}{2}}}\left\{\frac{Kb/2}{\left[\left(\frac{Kb}{2}\right)^2 + (2d)^2\right]^{\frac{1}{2}}}\right\}$$

$$w' = \frac{C\ c\ V\ (\frac{Kb}{2})}{4\pi\left[\left(\frac{Kb}{2}\right)^2 + (2d)^2\right]}$$

$$\epsilon = \frac{C_l\ c\ V\ (\frac{Kb}{2})}{4\pi\left[(\frac{Kb}{2})^2 + (2d)^2\right]}$$

$$\frac{d\epsilon}{dC_L} = \frac{c}{4\pi}\left[\frac{Kb/2}{(\frac{Kb}{2})^2 + (2d)^2}\right]$$

$$\frac{d\epsilon}{dC} \sim \frac{Kb/2}{(\frac{Kb}{2})^2 + (2d)^2}$$

Therefore, in proximity of the ground the change of downwash with respect to local lift coefficient is proportional to the following:

$$\left(\frac{\partial \epsilon}{\partial C_l}\right)_G \sim \left[\frac{1}{\frac{Kb}{2}} - \frac{Kb/2}{(\frac{Kb}{2})^2 + (2d)^2}\right]$$

By setting up a ratio between $\frac{\partial \epsilon}{\partial C_l}$ out of ground effect and $\frac{\partial \epsilon}{\partial C_l}$ in ground effect, the following equality is obtained:

$$\frac{\left(\frac{\partial \epsilon}{\partial C_l}\right)_G}{\left(\frac{\partial \epsilon}{\partial C_l}\right)} = \frac{1}{1 + (\frac{Kb}{4d})^2}$$

Aerodynamic texts state that for the lifting line theory of finite wings the trailing vortex filaments can be assumed to be 0.8 of the span apart. Substituting this value for K in the above equation yields:

$$\frac{\left(\frac{\partial \epsilon}{\partial C_l}\right)_G}{\left(\frac{\partial \epsilon}{\partial C_l}\right)} = \frac{1}{1 + 0.4\,(\frac{b}{d})^2}$$

The ratio of $\frac{\partial \epsilon}{\partial C_l}$ in ground effect to $\frac{\partial \epsilon}{\partial C_l}$ out of ground effect is only dependent upon wing span to height above ground, b/d. Therefore, a single curve utilizing the coordinates of the ratio of downwash versus b/d ratio can be constructed. This curve is shown in Figure 2.

For a finite aspect ratio wing, the lift coefficient is given as

$$C_L = 2\pi(\alpha - \alpha_i)$$

where α_i is the induced angle-of-attack which is equal to $\frac{C_L}{\pi A}$ for ellip-

tical lifting surfaces. Substituting this value into the above equation and taking the derivative with respect to α gives:

$$\frac{\partial C_L}{\partial \alpha} = \frac{2 \pi A}{A + 2}$$

By utilizing the same procedure as in the downwash effect, the following ratio of slope of the lift curves in and out of ground effect was obtained:

$$\frac{\left(\frac{\partial C_L}{\partial \alpha}\right)_G}{\left(\frac{\partial C_L}{\partial \alpha}\right)} = \frac{A + 2}{A + 2\left[\frac{1}{1 + 0.4 \left(\frac{b}{d}\right)^2}\right]}$$

For a particular aircraft with a wing of known aspect ratio, a plot of the ratio of the slope of lift curves versus b/d can be constructed. For the F-8 with an aspect ratio of 3.39, such a plot was obtained and is included as Figure 3.

Utilizing the curves of Figures 2 and 3, the coefficients in the equations of motion containing stability derivatives dependent on downwash or slope of lift curves of wing or tail were varied. The stability derivatives effected were X_α, Z_w, $M_{\dot{\alpha}}$, and M_α. The definitions of these derivatives in Appendix I were rearranged as shown in Appendix II in order to use the above derivation. Figures 4a, 4b, 4c, and 4d graphically present the value of these derivatives versus altitude above ground. The values of the coefficients containing these derivatives were then obtained and are presented in Figures 5a, 5b, 5c, and 5d.

The proximity of the ground on an aircraft causes a lowering of the drag polar, reduced drag level for lift attained. This effect was considered

offsetting the increased drag resulting from the increase of angle-of-attack during the flare maneuver. Therefore, the drag was assumed constant throughout this analysis.

6. Analog Construction for Complete Problem Simulation.

The equations of motion in dimensional form rearranged for analog simulation with necessary scaling factor notation included are:

$$a_u\bar{u} = -.0602a_u\bar{u} + \frac{X_\alpha}{m} a_\alpha \bar{\alpha} - 31.88a_\theta\bar{\theta} + .00145a_{\Delta T}\Delta\bar{T}$$

$$a_{\dot{\alpha}}\dot{\bar{\alpha}} = -.00113a_u\bar{u} + \frac{Z_w}{m}a_\alpha \bar{\alpha} + a_{\dot{\theta}}\dot{\bar{\theta}} - .0595\, a_\eta \bar{\eta}$$

$$a_{\ddot{\theta}}\ddot{\bar{\theta}} = 1.89 \times 10^{-4} a_u\bar{u} + \frac{M_{\dot{\alpha}}}{B} a_{\dot{\alpha}}\dot{\bar{\alpha}} + \frac{M}{B}a_\alpha \bar{\alpha} - .3396a_{\dot{\theta}}\dot{\bar{\theta}} - .455 \times 10^{-5} a_{\Delta T}\Delta\bar{T} - 2.504a_\eta\bar{\eta}$$

The scaling factors are included in Table III and the analog mechanization of the equations is shown in Figure 6.

The automatic-throttle transfer function given by Specialties, Inc. was converted into analog format as shown in Appendix III with the scaling factors included in Table III and then mechanized. The analog mechanization is shown in Figure 7.

For the complete problem simulation, auxiliary equations for generating actual altitude during the approach, glide slope and acceleration normal to the glide slope in "g" units were derived as shown in Appendix IV with scaling factors also included in Table III. The equations

were mechanized as represented in Figure 8. These equations in analog format are:

Altitude:

$$a_H \bar{H} = a_{H_o} \bar{H}_o - \gamma_o(\text{rad}) \int a_{u_o} \bar{U}_o + (a_{u_o} \bar{U}_o + a_u \bar{u}) \int a_\gamma \bar{\gamma}$$

Glide slope:

$$a_\gamma \bar{\gamma} = a_\theta \bar{\theta} - a_\alpha \bar{\alpha}$$

Acceleration:

$$a_n \frac{\bar{n}}{g} = \frac{1}{g} (a_{u_o} \bar{U}_o + a_u \bar{u})(a_{\dot{\theta}} \dot{\bar{\theta}} - a_{\dot{\alpha}} \dot{\bar{\alpha}})$$

To perform the flare maneuver, an analog mechanization for elevator control was constructed by applying a steady voltage through a potentiometer to an integrator amplifier circuit. Thus, by adjusting the potentiomenter, application of step input or variable slope ramp input of elevator to the airframe could be obtained. The elevator circuit was further controlled by an off/on function switch built into the Donner computer.

7. Experimental Methods and Results.

7.1 Ground Effect Investigation.

Due to an insufficient number of available amplifiers on the Donner Analog Computer for the simulation required in this study, it was impossible to include all the ground effect variables. Therefore, it was necessary to evaluate the influence of each variable on the dynamic stability of the basic airframe inorder that a simplification could be obtained. Prior to experimentation, it was concluded that ground effect acting on the derivative M_α would be the most influential and therefore would be retained.

A dynamic stability analysis on the airframe equations of motion without forcing functions of thrust and elevator was performed. Using initial condition of $u(0) = 25$ ft./sec. for the phugoid determination and an initial condition of $\alpha(0) = 5$ degrees for the short period mode of motion determination, the following analog runs were obtained:

(1) Time histories of α and u perturbations out of ground effect included as Figure 9.

(2) Time histories of α and u perturbations with all ground effect variables included for heights above ground corresponding to b/d ratios 1.0, 2.0, 3.0, and 4.0. Results are included as Figure 10.

(3) Time histories of α and u perturbations neglecting ground effect on derivatives X_α and Z_w for the same altitudes as in (2). The analog run outs are included in Figure 11.

(4) Time histories of α and u perturbations neglecting ground effect on derivatives X_α, Z_w, and $M_{\dot{\alpha}}$ for the same altitudes as before. The analog representations are included in Figure 12.

Analysis of Figure 9 determined that the phugoid period is 34 seconds and that of the short period mode is six seconds. Times to damp to $\frac{1}{2}$ amplitude are approximately 30 seconds and 2 seconds respectively. With the condition of all variables included, the maximum deviation from the no ground effect analysis in the phugoid and short period modes was 0.3 seconds. There was no noticeable change in the times to damp $\frac{1}{2}$ amplitude. Analysis of the analog runs when holding X_α and Z_w constant showed no noticeable change of period or time to damp to $\frac{1}{2}$ amplitude of

either mode of motion from those obtained with all derivatives variable. When the derivatives $M_{\dot{\alpha}}$, Z_w, and X_α were held constant, the phugoid mode period was 0.2 seconds longer and the short period's 0.1 seconds shorter then obtained when varying all the derivatives. The times to damp to $\frac{1}{2}$ amplitude were basically unchanged.

Since the relative influence of the variable derivatives X_α, Z_w, and $M_{\dot{\alpha}}$ on the dynamic stability was inconsequential, the decision was made to conduct the investigation of this study with these three derivatives invariant to ground effect. The derivative M_α which was retained as a variable dependent on altitude was constructed on a function generator for analog use. The analog mechanization is shown in Figure 13.

7.2 Design Auto-throttle System Operation.

The normal auto-throttle system with and without ground effect was investigated to insure proper analog mechanization prior to commencing experimentation for the proposed system during the flare maneuver. Analog runs with auto-throttle operating for initial conditions of horizontal gusts, $u(0) = +5$ knots, vertical gusts, $\alpha(0) = 5^o$, and pitch angle $\theta(0) = +4^o$.

Figure 14a shows the response obtained without ground effect for an initial horizontal gust. The velocity perturbation is oscillatory damped with an initial overshoot approximately 45% of u(0) and was without a second overshoot. Figure 14b is the response for an initial horizontal gust with ground effect and agrees closely with that of no ground effect. The thrust application is oscillatory in both cases with a damped wave motion with a peak $\Delta T =$

1200 lb.

Figures 15a and 15b present the response obtained for an initial vertical gust with and without ground effect respectively. The oscillatory velocity perturbation is rapidly damped with an oscillatory throttle application with a peak $\Delta T = 6,300$ lb.

The analog results for the initial pitch angle condition without ground effect is presented in Figure 16. The velocity perturbation is postively damped with a slight oscillatory tendency which is always negative. The thrust application is smoother than in the other initial conditions and has a peak $\Delta T = 600$ lb.

The results obtained for the design application investigated correspond to the results obtained in Ref. 1 and are as expected. The analog mechanization was therefore considered correct. The numerical forms of all the equations are as in Appendices I - IV and the analog potentiometer settings is included as Appendix V.

7.3 Elevator Angle for Flare Maneuver.

The elevator deflection required to perform the flare maneuver was approximated from the equation given in Ref. 5 relating the elevator angle per "g" for a constant acceleration maneuver. This equation is:

$$\frac{\Delta \eta}{n - 1} = \frac{C_{m_\alpha} C_L + \frac{g}{V} C_{mq} C_{L_\alpha}}{C_{L_\alpha} C_{m_\eta} - C_{m_\alpha} C_{L\eta}}$$

Substituting in the required values for the non-dimensional derivatives and an average normal acceleration of 1.1 g, the resulting elevator deflection

was approximately - 2.7 degrees.

Since a pilot will normally pull a maximum of + 0.2 g above the steady state 1 g during flare, the rate of elevator application was obtained by adjusting the potentiometer in the elevator circuit until a peak "g" perturbation of 0.2 g was obtained.

Thus, elevator was applied at the required rate until a total of - 2.7^{o} was obtained or touchdown occurred.

7.4 Determination of Auto-Throttle Supplementary Circuit.

In order to obtain an insight as to what commands the supplementary circuit shall supply the design auto-throttle system, analog runs of a flare maneuver with constant thrust and with the design system operating were performed. The constant thrust response is shown in Figure 17. The velocity is seen to decrease 18 ft./sec. during the flare maneuver. The response obtained while the auto-throttle was operating is shown in Figure 18. The velocity decreases initially then attempts to return to the beginning steady state velocity as a result of an increase of thrust.

The above results indicated that the additional commands prescribed for the auto-throttle supplementary circuit must effectively cancel the commands that caused the thrust to increase.

The analog mechanization of the two biasing commands, as discussed in Section 3, is shown in Figure 19. To simulate real system operation, the same gains were used in the angle-of-attack bias, α_{B}, and normal acceleration bias, g_{B}, as in the original APC system; however, an additional

potentiometer was inserted in each circuit inorder to control the amount of α_B or g_B sent to the auto-throttle block. The biasing command could then be comprised of both α_B and g_B or either one of them.

Analog experimentation for determining the bias commands was performed as follows:

(1) Biasing only the normal acceleration loop through a range of 0.2 g to 0.01 g.

(2) Biasing only the α loop through the range of $0.01\,\Delta\eta$ to $1.0\,\Delta\eta$.

(3) Biasing both the α and "g" loops through their respective ranges.

The responses for the normal acceleration biasing were initial decreases in airspeed to a minimum value followed by an increase. The minimum velocity was never less than 224 ft./sec. regardless of the amount of g_B as an increase of thrust was always obtained. The aircraft's motion was a pull up with a variable minimum altitude dependent on amount of g_B. A representative record of the typical response obtained is included as Figure 20 which is the run with $g_B = -0.02$ g.

The typical response obtained when biasing only the angle-of-attack loop was a smooth decrease in velocity to a minimum followed by a slight increase to a new steady state value. The angle-of-attack increased rapidly to a peak angle then decreased to a damped perturbation about some median angle. The thrust was decreased initially by a maximum of three to four thousand pounds depending on the amount of bias and then began increasing as the flare continued. As α_B was increased, a greater decrease in

velocity and higher peak angle-of-attack were attained. With the described elevator application, an α_B of 0.802η resulted in a smooth velocity decrease of 25 ft./sec. to the desired 209 ft./sec. at the touchdown point. Touchdown occurred seven seconds after flare was commenced but the vertical kinetic energy was not completely dissipated as a slight vertical velocity component was evidenced in the altitude read out. The peak angle-of-attack = 3.8° occurred at an altitude of 20 ft. and the maximum thrust decrease was 3000 lb. This presentation is included as Figure 21.

The results obtained during the analog runs while biasing both the angle-of-attack and normal acceleration loops indicated that the airspeed response could be more advantageously controlled. Also, the magnitude changes in thrust were less than those obtained in the α_B condition. The peak angles-of-attack were also decreased along with their rate of increase. The airspeed increased slightly as the flare was commenced then smoothly decreased to a minimum value. This minimum velocity was followed by a damped perturbation about a velocity approximately four ft./sec. greater than the minimum. With the elevator application as previously stated, an optimum condition was obtained with $\alpha_B = .805\eta$ and $g_B = -.15g$. This bias condition resulted in the smoothest decrease in velocity to a minimum 209 ft./sec. that occurred exactly at the touchdown point. The flare was a smooth manuever with essentially all the vertical kinetic energy being dissipated. The peak angle-of-attack = 3.3° occurred 6.5 sec. after flare commenced and 3.2 sec. prior to touchdown. The thrust increased initially to a peak of + 400 lb. then decreased to a minimum - 2200 lb. and finally

increased to a positive 1000 lb. above the beginning steady state value.

8. Summary of Analog Results and Recommendations.

The analog experimentation disclosed that a desired reduction of velocity could be obtained during the flare maneuver. Two different supplementary circuits to the design auto-throttle produced a required touchdown velocity with a simplified elevator application. These circuits were comprised of (a) biasing only the angle-of-attack loop by a percentage of the ramp elevator application, and (b) biasing both the angle-of-attack and normal acceleration loops with a percentage of the elevator and a constant value of "g" respectively.

The α_B produced a smoother throttle response; however, it had a greater magnitude change of thrust. This bias also caused a more rapid α change and a greater peak α while not dissipating all the vertical kinetic energy. The energy could be dissipated by changing the elevator deflection but the desired airspeed response could not be attained. The circuit comprised of biasing both loops had a less smooth thrust response with a very slight velocity increase initially. The flare maneuver was smoother with essentially all the vertical kinetic energy dissipated. The rate of α increase was improved and a less peak α was obtained.

In general, the supplementary circuit entailing biasing both auto-throttle input loops produces better aircraft response even though the thrust application was not as smooth. Further investigation to obtain an optimum supplementary circuit is required when all the ground effect variables are

included along with the changes in the lift and drag coefficients resulting from the increased angle-of-attack during the flare. An analysis in system operation with gusts during the flare maneuver and the associated elevator application is also required.

It is recommended that the required further analyses be performed on a hybrid simulator consisting of analog and digital computers. These additional analyses could not be performed in this study as the Donner 3100 Analog Computer was completely saturated.

9. Conclusions and Acknowledgements.

1. The use of the auto-throttle device with sensed inputs of angle-of-attack and acceleration normal to the glide slope for field landings with a flare maneuver is determined feasible.

2. The throttle could be controlled to produce a reduction of airspeed during the flare to a desired minimum at touchdown together with zero rate of descent.

3. The desired results were accomplished by incorporating a supplementary circuit, energized during the flare maneuver, in the design auto-throttle system. This circuit would be comprised of an angle-of-attack rate command to a maximum and a constant signal command of normal acceleration.

4. As might be expected, system functioning appeared to be critically dependent upon the rate of application of elevator during the flare.

The writer wishes to express his gratitude to Professor E. J. Andrews, Department of Aeronautics, U. S. Naval Postgraduate School, for his technical assistance and encouragement in the preparation of this study.

BIBLIOGRAPHY

1. Bell, G. R. An Investigation of the Effect of Auto-Throttle Devices on Aircraft Control in the Carrier Landing Approach. U. S. Naval Postgraduate School, 1963 - B 360.

2. Evans, R. E. and Schuppe, R. H. An Investigation of the Effect of Simplified Equations of Motion and Various Inputs on Automatic-Throttle Devices. U. S. Naval Postgraduate School, 1964 - E 775.

3. Anon. Comparison of Two Automatic-Throttle Controllers for the F8 U-2N Aircraft. U. S. Naval Air Development Center. Report No. NADC - ED - LG 292, 1962.

4. Anon. Criteria for Predicting Landing Approach Speed Based on an Analog Computer Analysis of 21 Jet Propelled Aircraft. Vought Aeronautics, Report No. EOR - 13202, 1960.

5. Etkin, B. Dynamics of Flight. John Wiley and Sons, Inc., 1959.

TABLE I

LONGITUDINAL STABILITY DERIVATIVE VALUES

$X_u = -41.14 \quad \frac{\text{lb.}}{\text{ft./sec.}}$

$X_w = -9.71 \quad \frac{\text{lb.}}{\text{ft./sec.}}$

$X_\alpha = -2272.14 \quad \text{lb.}$

$X_{\Delta T} = 0.99 \quad \frac{\text{lb.}}{\text{ft./sec.}}$

$Z_u = -181.69 \quad \frac{\text{lb.}}{\text{ft./sec.}}$

$Z_w = -291.85 \quad \frac{\text{lb.}}{\text{ft./sec.}}$

$Z_\eta = -9522.04 \quad \text{lb.}$

$M_u = 18.15 \quad \text{lb.-sec.}$

$M_{\dot{\alpha}} = -3940.41 \quad \text{ft.-lb.-sec.}$

$M_\alpha = -109,377.45 \quad \text{ft.-lb.}$

$M_q = -32,602.94 \quad \text{ft.-lb.-sec.}$

$M_{\Delta T} = -0.437 \quad \text{lb.-sec.}$

$M_\eta = 240,342.91 \quad \text{ft.-lb.}$

TABLE II

F-8 AIRCRAFT PARAMETERS

U_o = 234 ft./sec.	C_{D_u} = 0.0
c.g. = 24% MAC	C_{L_α} = 2.598
W = 22,000 lb.	C_{L_η} = 0.3897
α_o = 8.1°	C_{m_u} = 0.738 X 10^{-2}
θ_o = 4.1°	C_{m_α} = - 0.38
S_w = 375 ft^2.	$C_{m_{\dot{\alpha}}}$ = - 0.55
S_T = 93.4 ft^2.	$C_{L_{\alpha_T}}$ = 1.622
b = 35.666 ft^2.	h = 0.24
l_t = 14.081 ft.	$h_{n_{wb}}$ = 0.293
$\bar{c}$ = 11.78 ft.	$C_{L_{\alpha_{wb}}}$ = 2.387
C_L = 0.87	$\frac{d\epsilon}{d\alpha}$ = 0.4772
C_D = 0.197	A = 3.39
C_{D_α} = 0.963	

TABLE III

ANALOG SCALING FACTORS

Maximum Voltage 100 volts

u: 100 v. = 50 ft./sec. ; a_u = 0.5 ft./sec.-v.

$\dot{u}$: 100 v. = 50 ft./sec^2. ; $a_{\dot{u}}$ = 0.5 ft./sec^2.-v.

α: 100 v. = 10^o = .1745 rad. ; a_α = 0.1^o/v. = .001745 rad/v.

$\dot{\alpha}$: 100 v. = 10^o/sec. = .1745 $\frac{\text{rad.}}{\text{sec.}}$; $a_{\dot{\alpha}}$ = .1 $\frac{\text{deg}}{\text{sec.-v.}}$

θ: 100 v. = 20^o = .349 rad. ; a_θ = .2^o/v. = .00349 rad/v.

$\dot{\theta}$: 100 v. = 20^o/sec. = .349 $\frac{\text{rad.}}{\text{sec.}}$; $a_{\dot{\theta}}$ = .2^o/sec-v. = .00349 $\frac{\text{rad.}}{\text{sec-v.}}$

$\ddot{\theta}$: 100 v. = 20^o/sec^2 = .349 $\frac{\text{rad}}{\text{sec}^2}$; $a_{\ddot{\theta}}$ = .2^o/sec^2-v. = .00349 $\frac{\text{rad}}{\text{sec}^2}$-v.

γ: 100 v. = 20^o = .349 rad. ; a_γ = .2^o/v. = .00349 rad/v.

n: 100 v. = 2 g ; a_n = .02 g/v.

U_o: 100 v. = 300 ft./sec. ; a_{U_o} = 3.0 ft./sec.-v.

ΔT: 100 v. = 8000 lb. ; $a_{\Delta T}$ = 80 lb./v.

η: 100 v. = 28.65^o = .5 rad. ; a_η = 28.65^o/v. = .005 rad./v.

$\frac{M_\alpha}{B}$: 100 v. = 2.0 /sec^2. ; $\frac{a_{M_\alpha}}{B}$ = .02 /sec^2-v.

H: 100 v. = 300 ft. ; a_H = 3.0 ft./v.

FIGURE 1

BLOCK DIAGRAM OF AUTO-THROTTLE SYSTEM

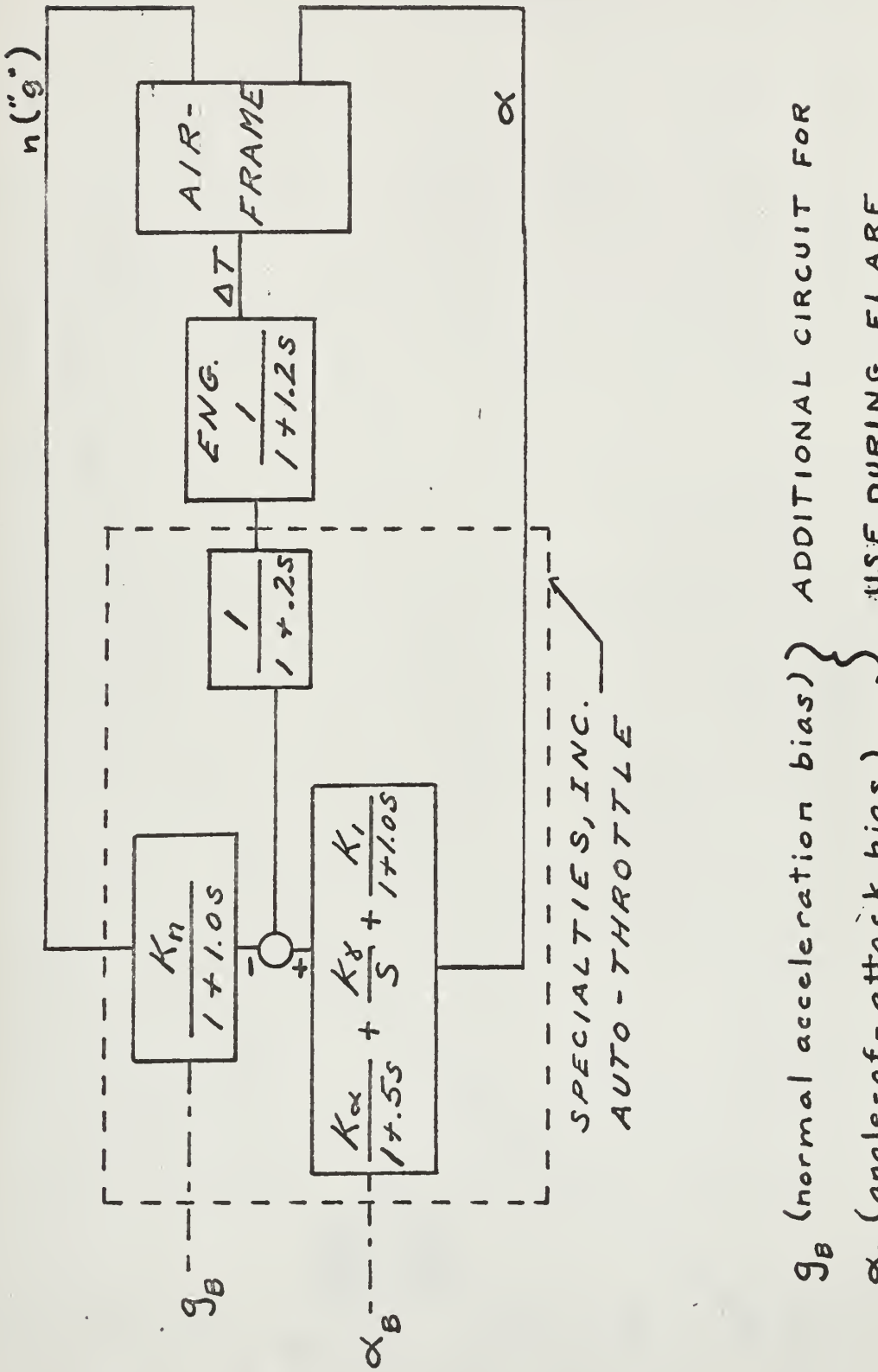

FIGURE 2

GROUND EFFECT ON

DOWNWASH AT TAIL

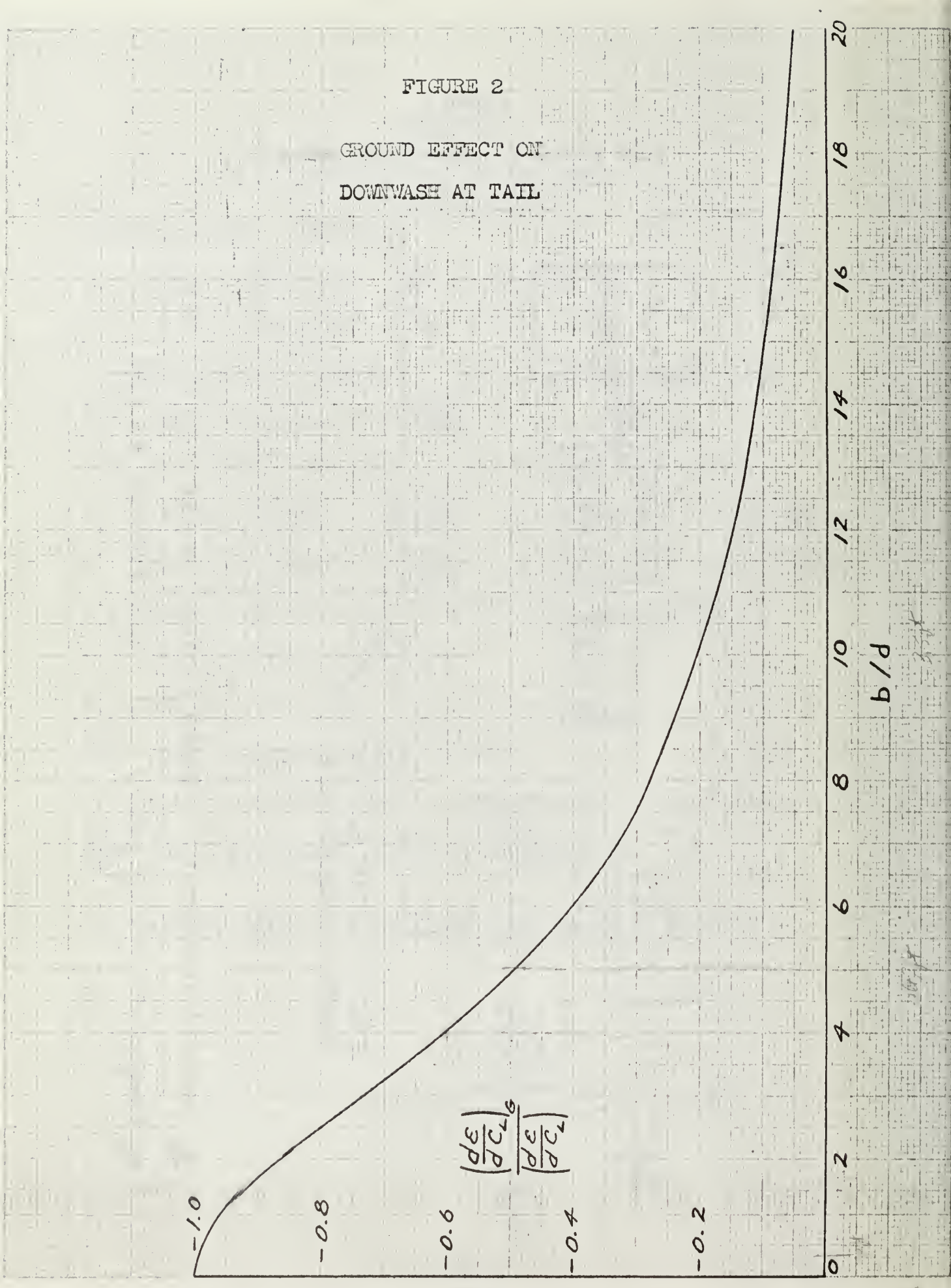

FIGURE 3

GROUND EFFECT ON LIFT CURVE SLOPE

FIGURE 4a

STABILITY DERIVATIVE X_α

WITH GROUND EFFECT

FIGURE 4b

STABILITY DERIVATIVE Z_w

WITH GROUND EFFECT

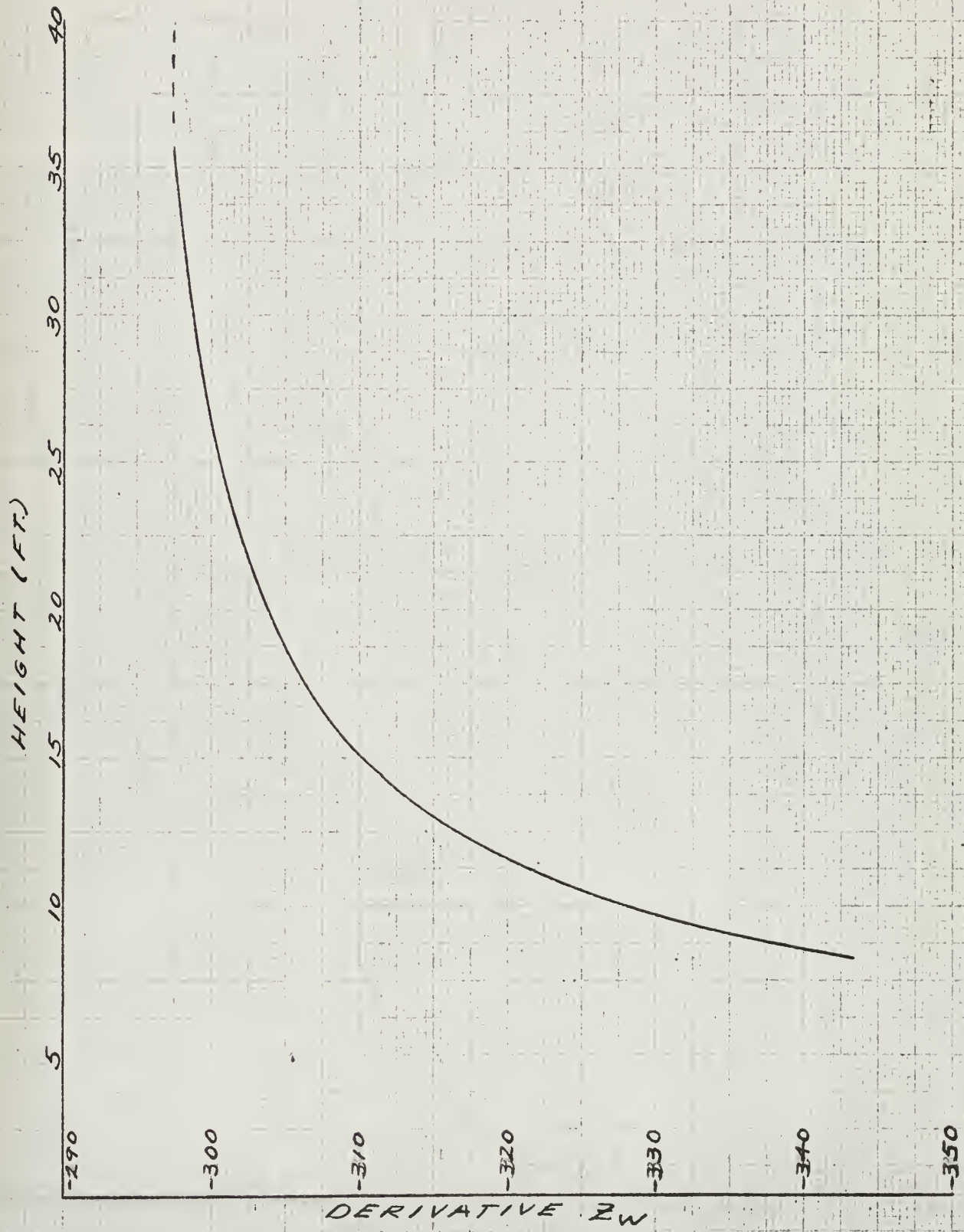

FIGURE 4c

STABILITY DERIVATIVE $M_{\dot{\alpha}}$

WITH GROUND EFFECT

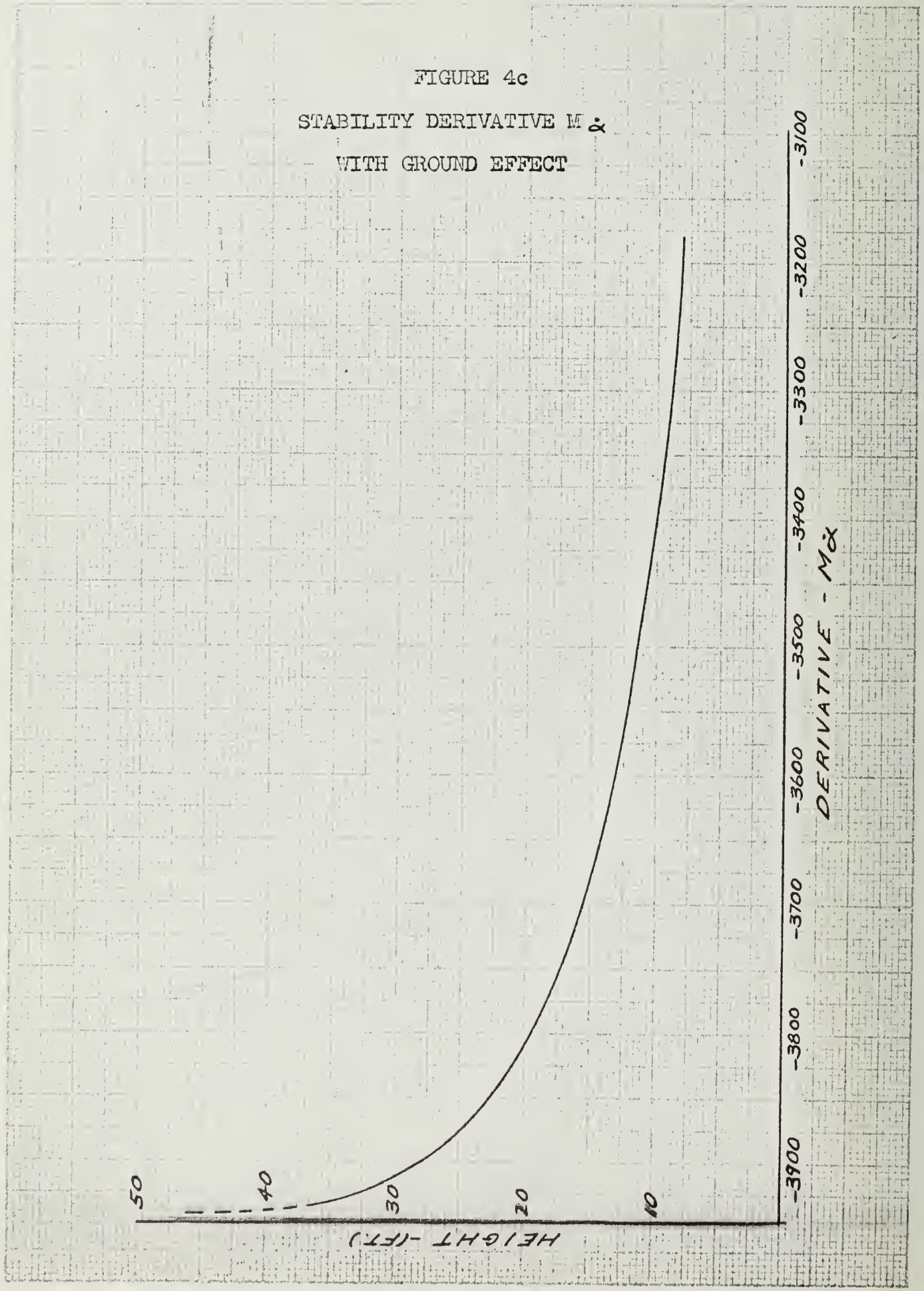

FIGURE 4d

STABILITY DERIVATIVE M_α

WITH GROUND EFFECT

FIGURE 5a

COEFFICIENT $\frac{X_\alpha}{m}$ WITH

GROUND EFFECT

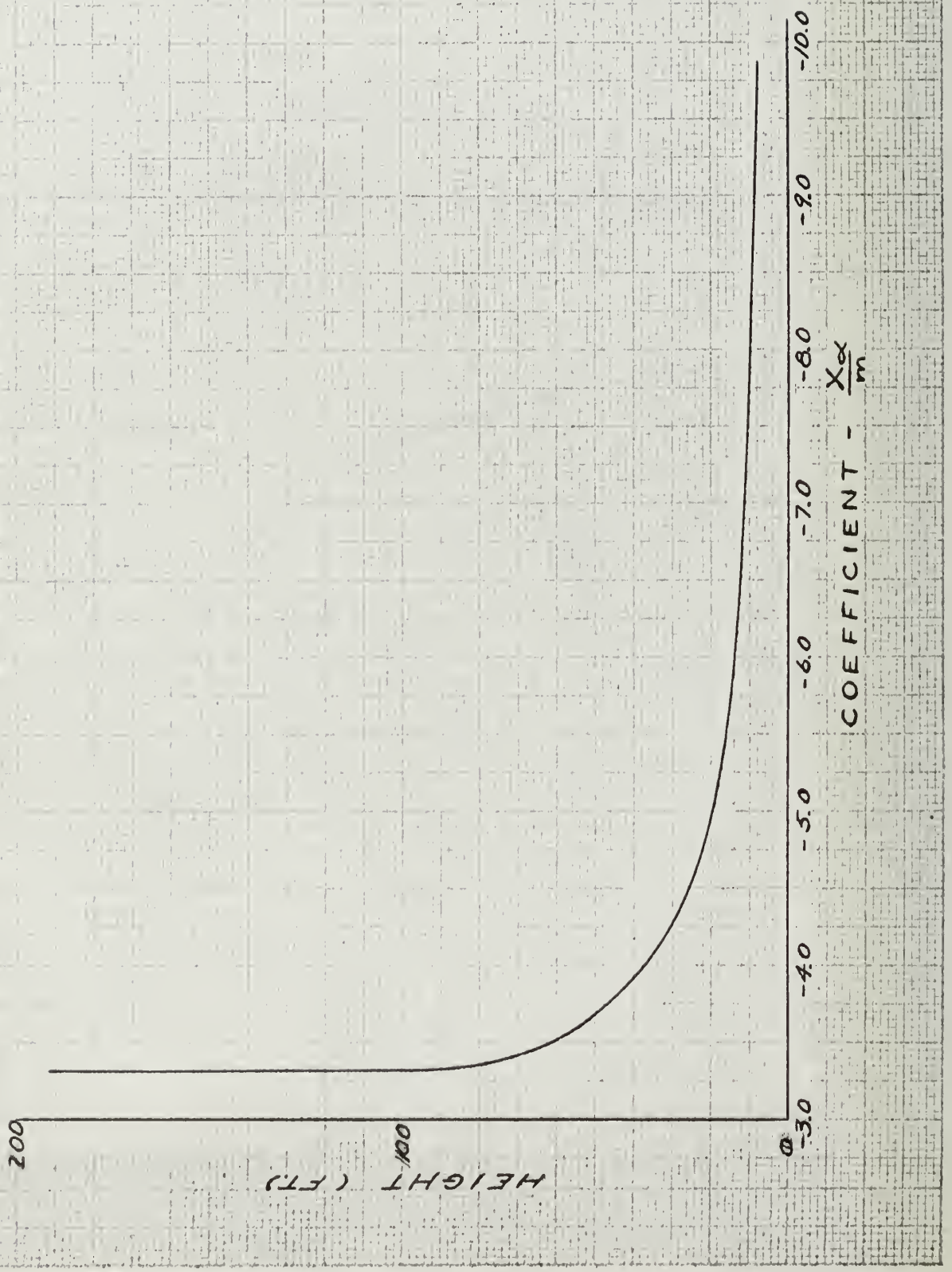

FIGURE 5b

COEFFICIENT $\frac{Z_w}{m}$ WITH

GROUND EFFECT

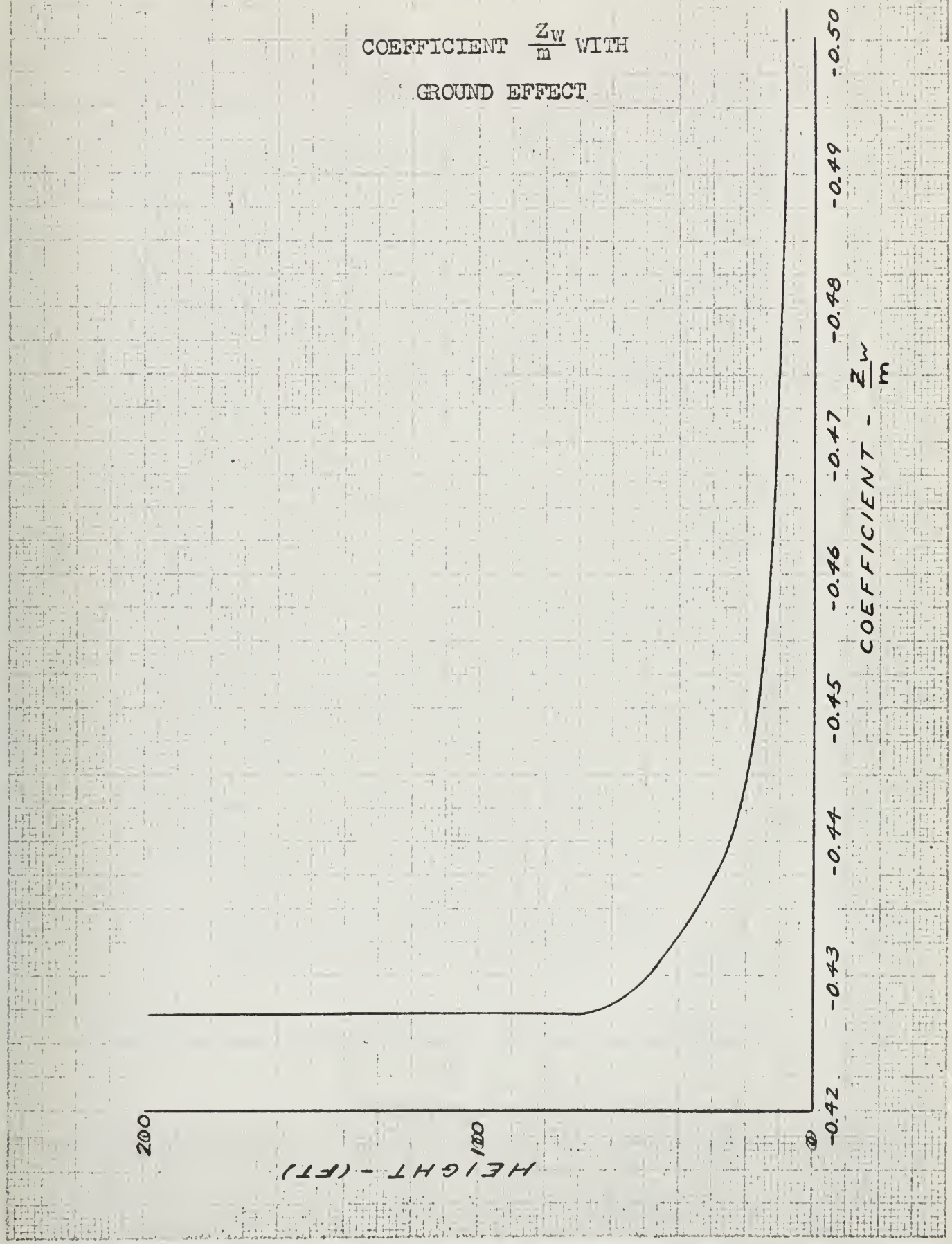

FIGURE 5c

COEFFICIENT $\frac{M_{\dot{\alpha}}}{B}$ WITH

GROUND EFFECT

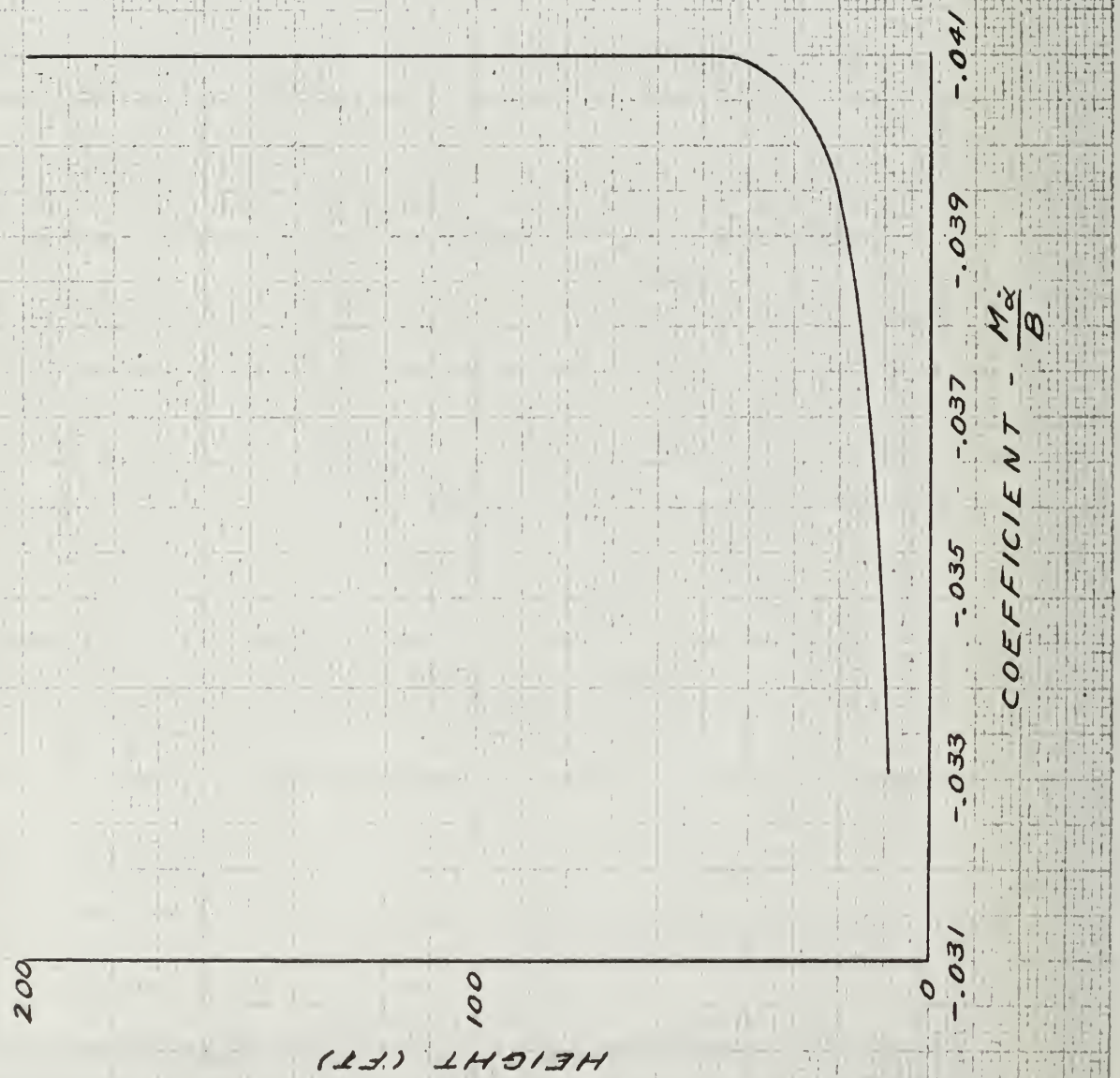

FIGURE 5d

COEFFICIENT $\frac{M_\alpha}{B}$ WITH

GROUND EFFECT

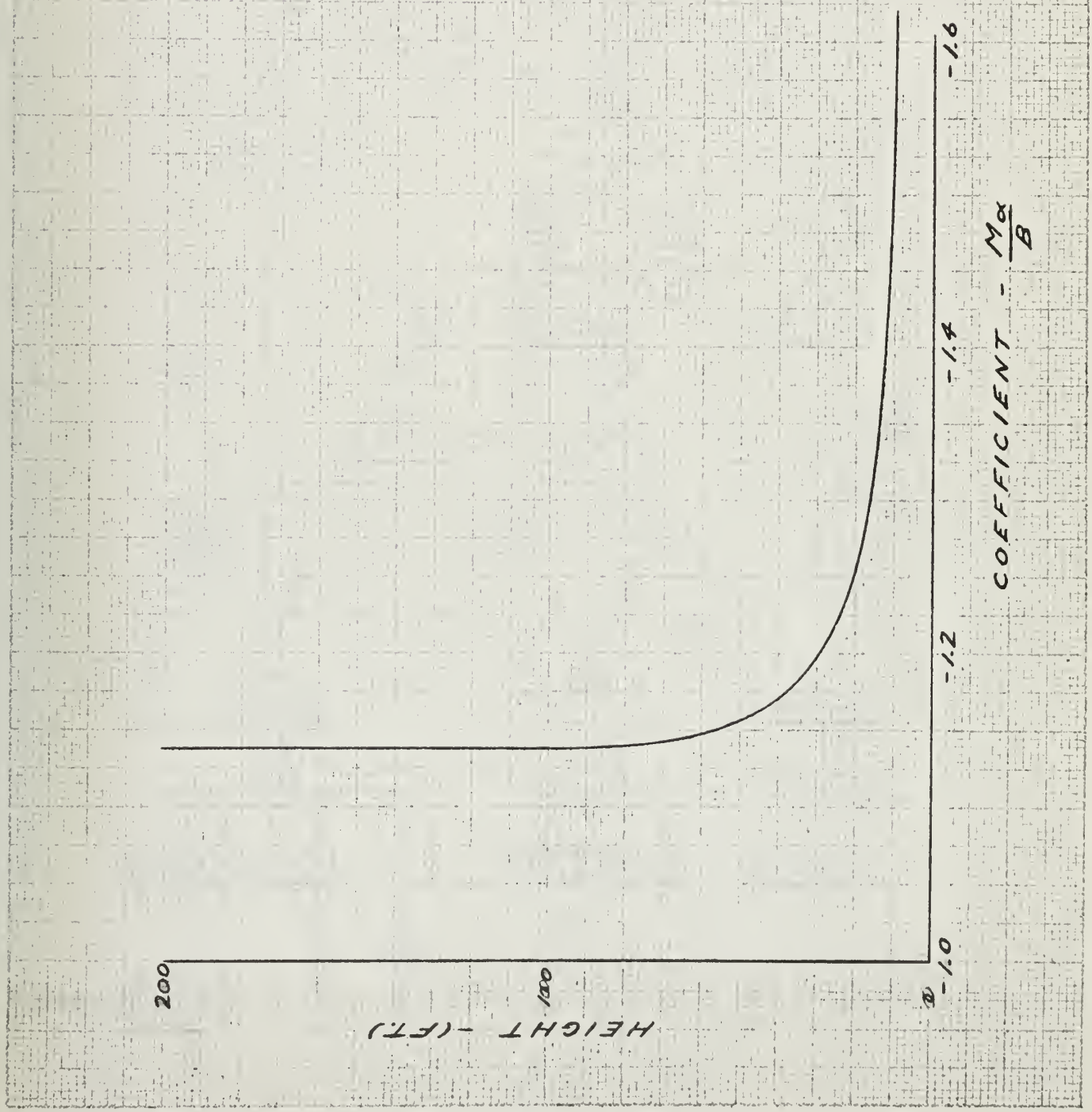

FIGURE 6

ANALOG MECHANIZATION OF

EQUATIONS OF MOTION

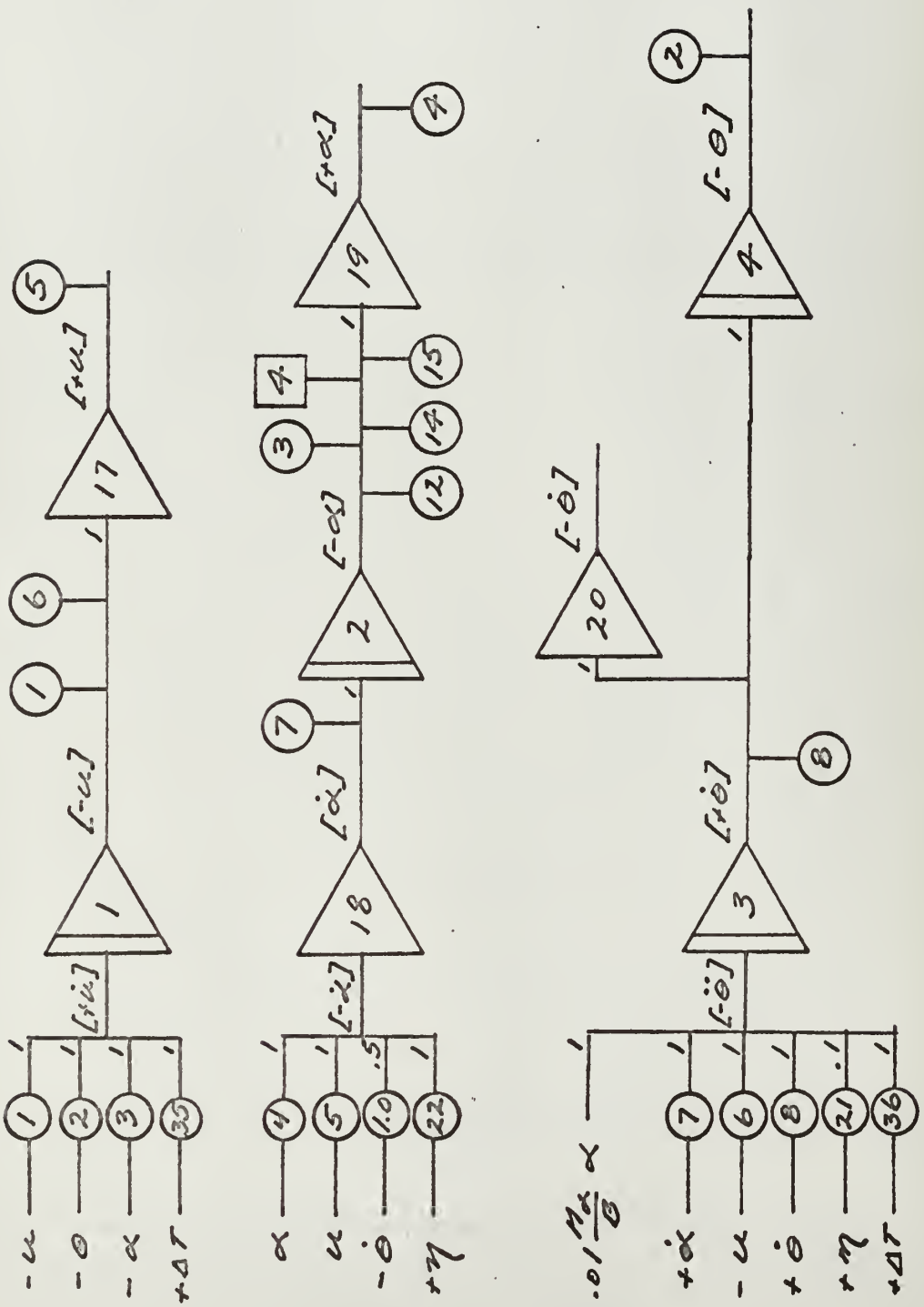

FIGURE 7

ANALOG MECHANIZATION OF

AUTO-THROTTLE BLOCK

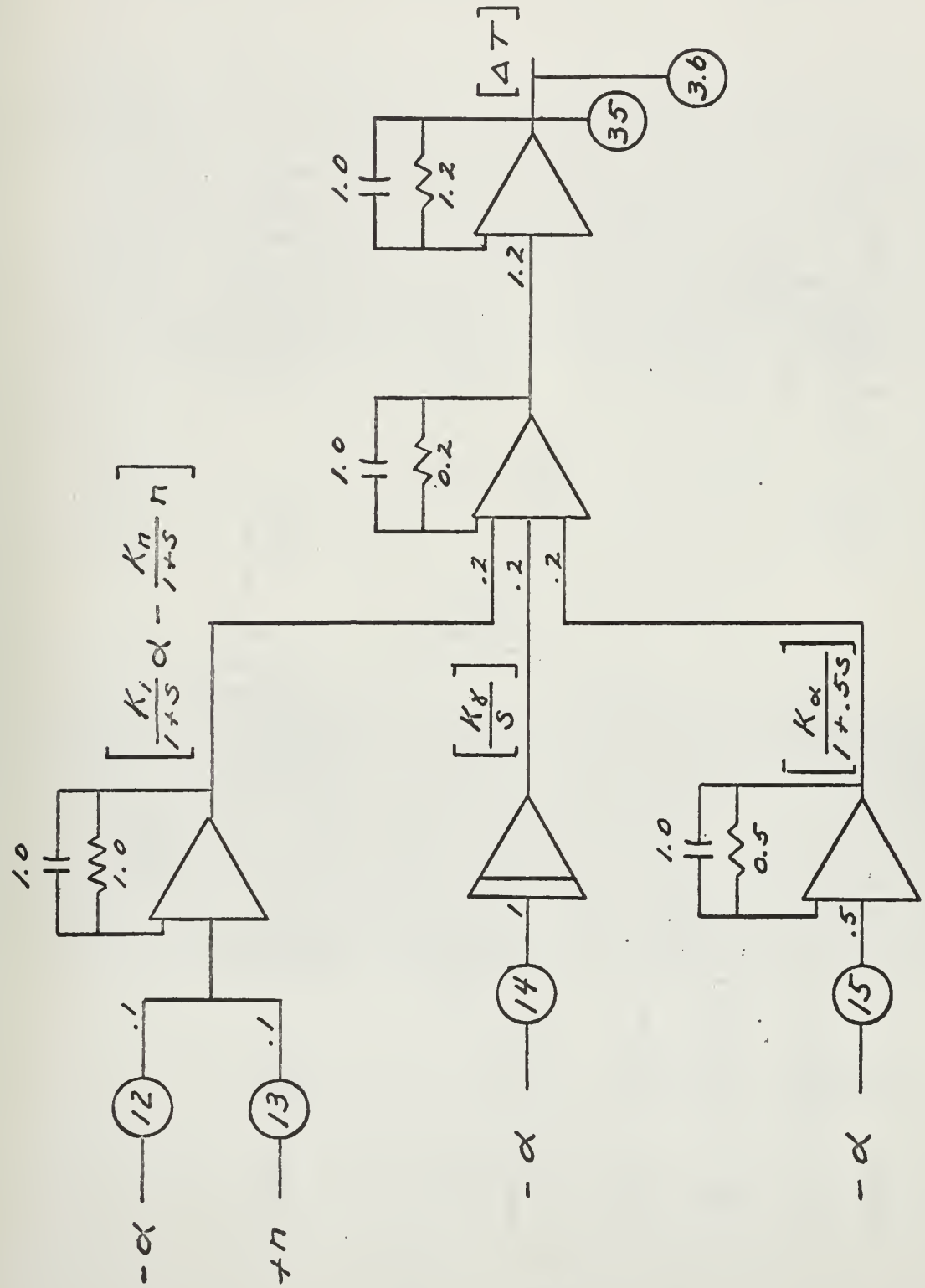

FIGURE 8

ANALOG MECHANIZATION OF

AUXILIARY EQUATIONS

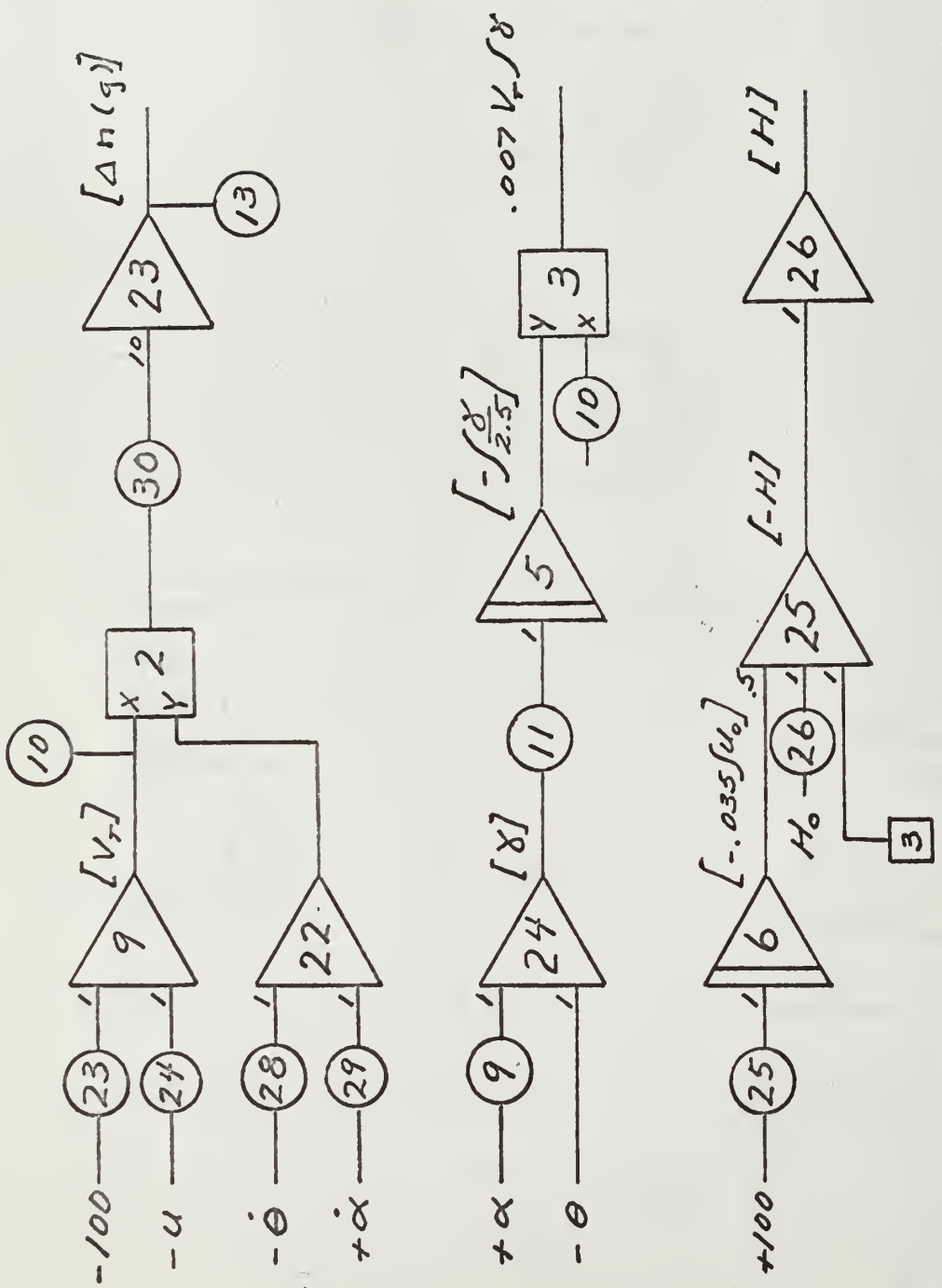

FIGURE 9

AIRFRAME STABILITY ANALYSIS

NO GROUND EFFECT

PHUGOID MODE

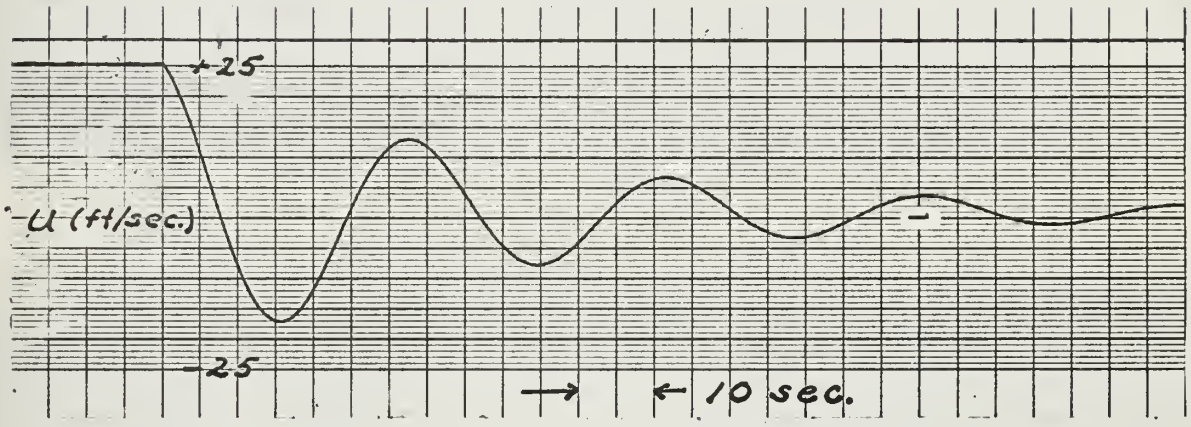

SHORT PERIOD MODE

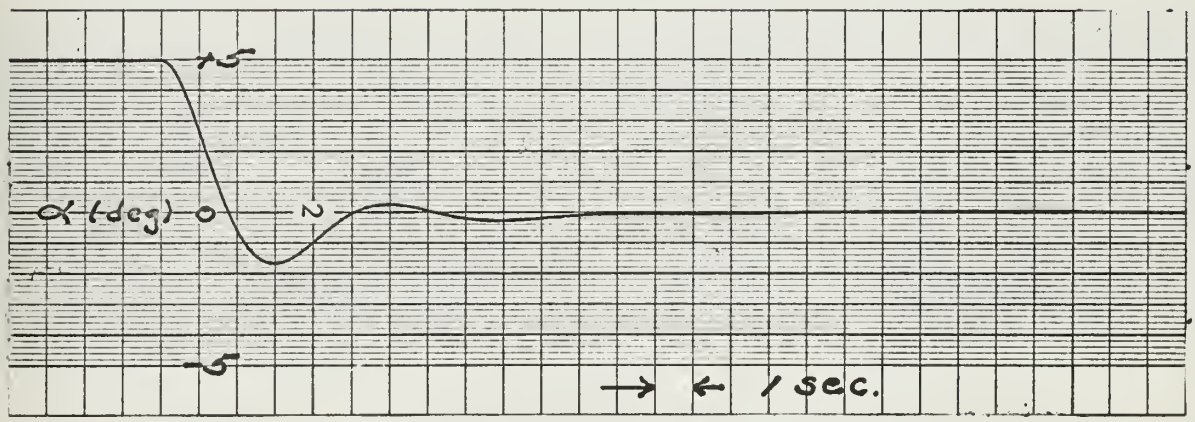

FIGURE 10
AIRFRAME STABILITY ANALYSIS
DERIVATIVES X_α, Z_w, M_α, $M_{\dot{\alpha}}$ VARIABLE

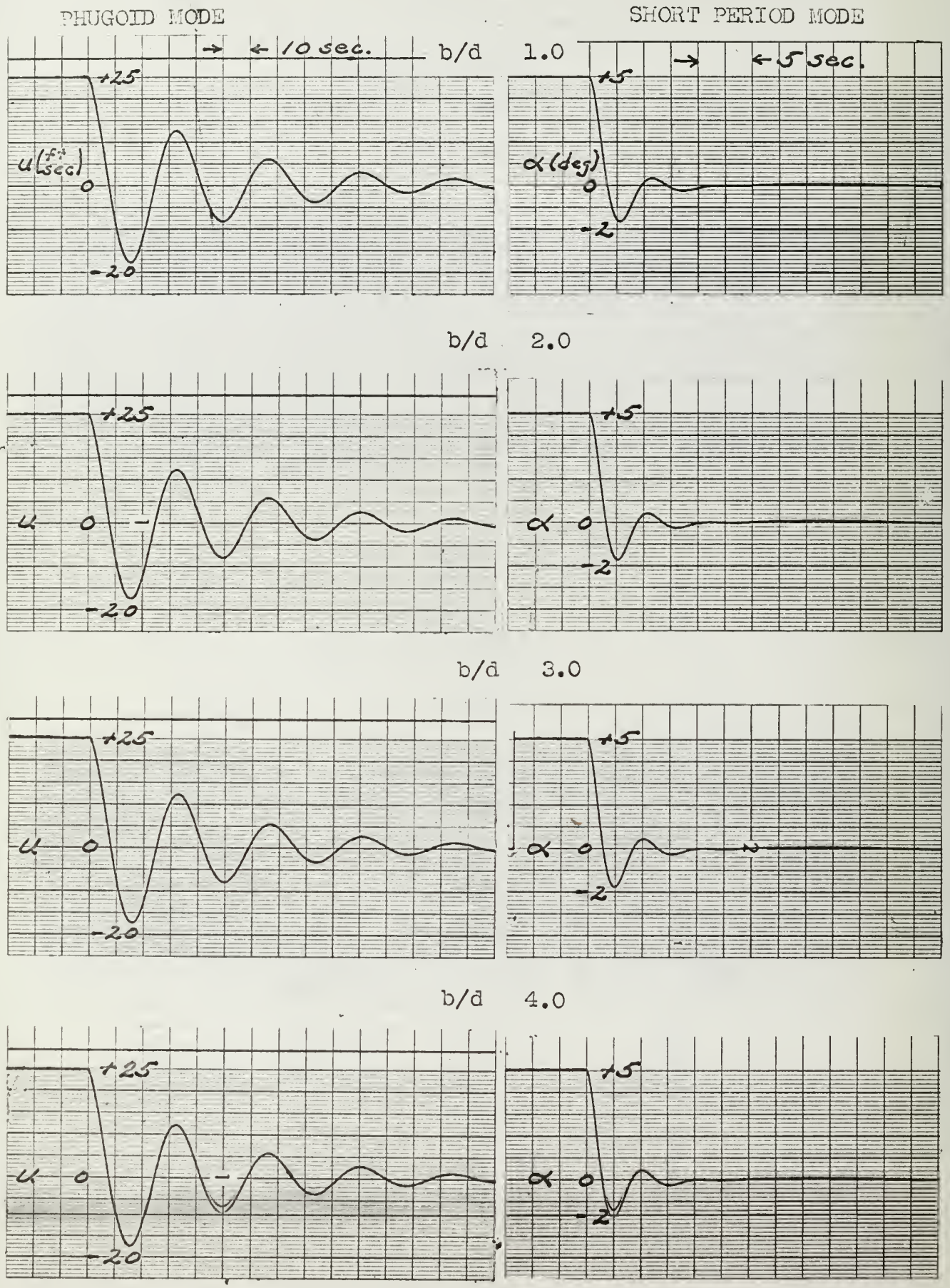

FIGURE 11
AIRFRAME STABILITY ANALYSIS
DERIVATIVES X_α, M_α VARIABLE

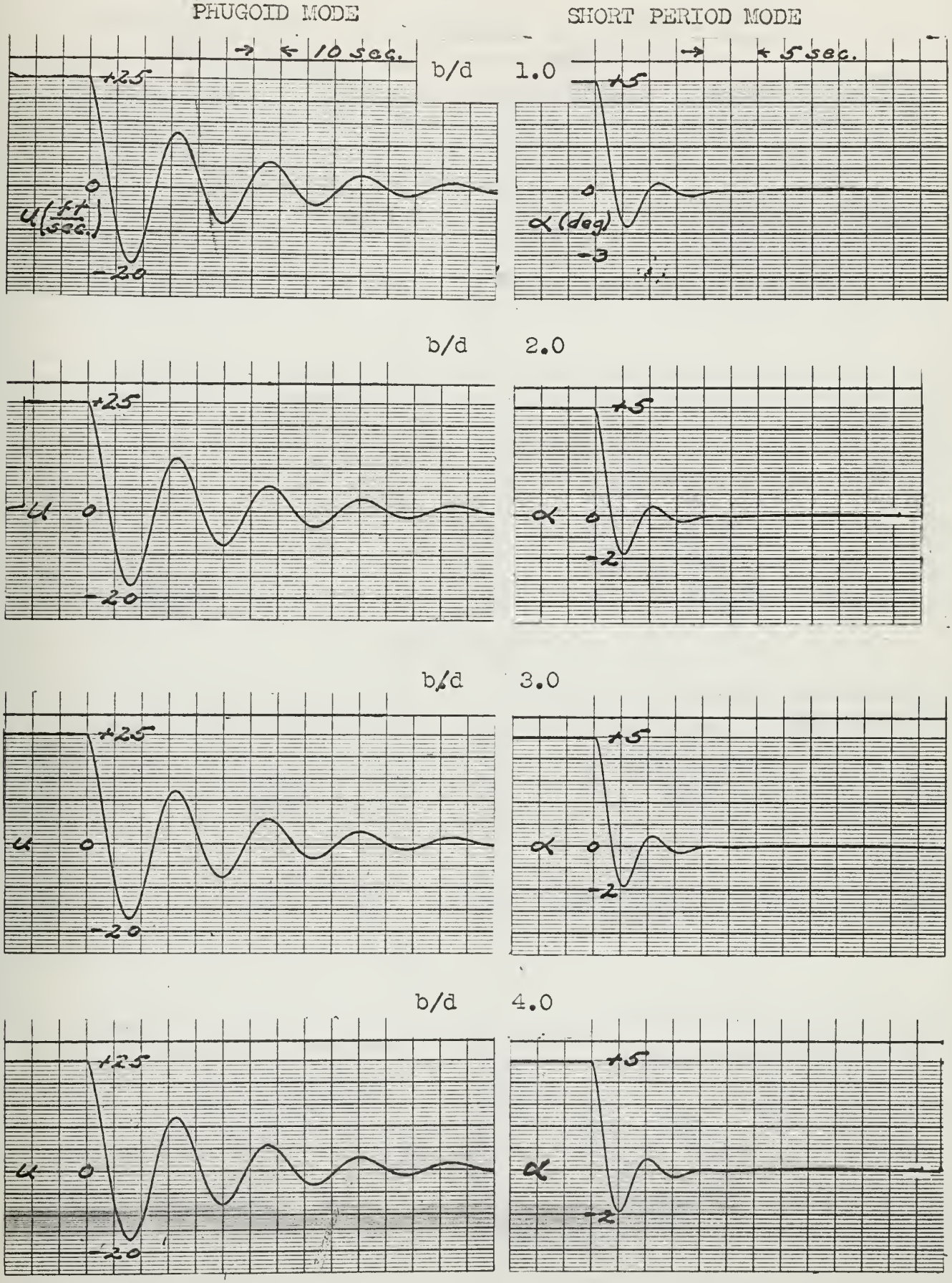

FIGURE 12
AIRFRAME STABILITY ANALYSIS
DERIVATIVES X_α, Z_w, $M_{\dot{\alpha}}$ INVARIANT

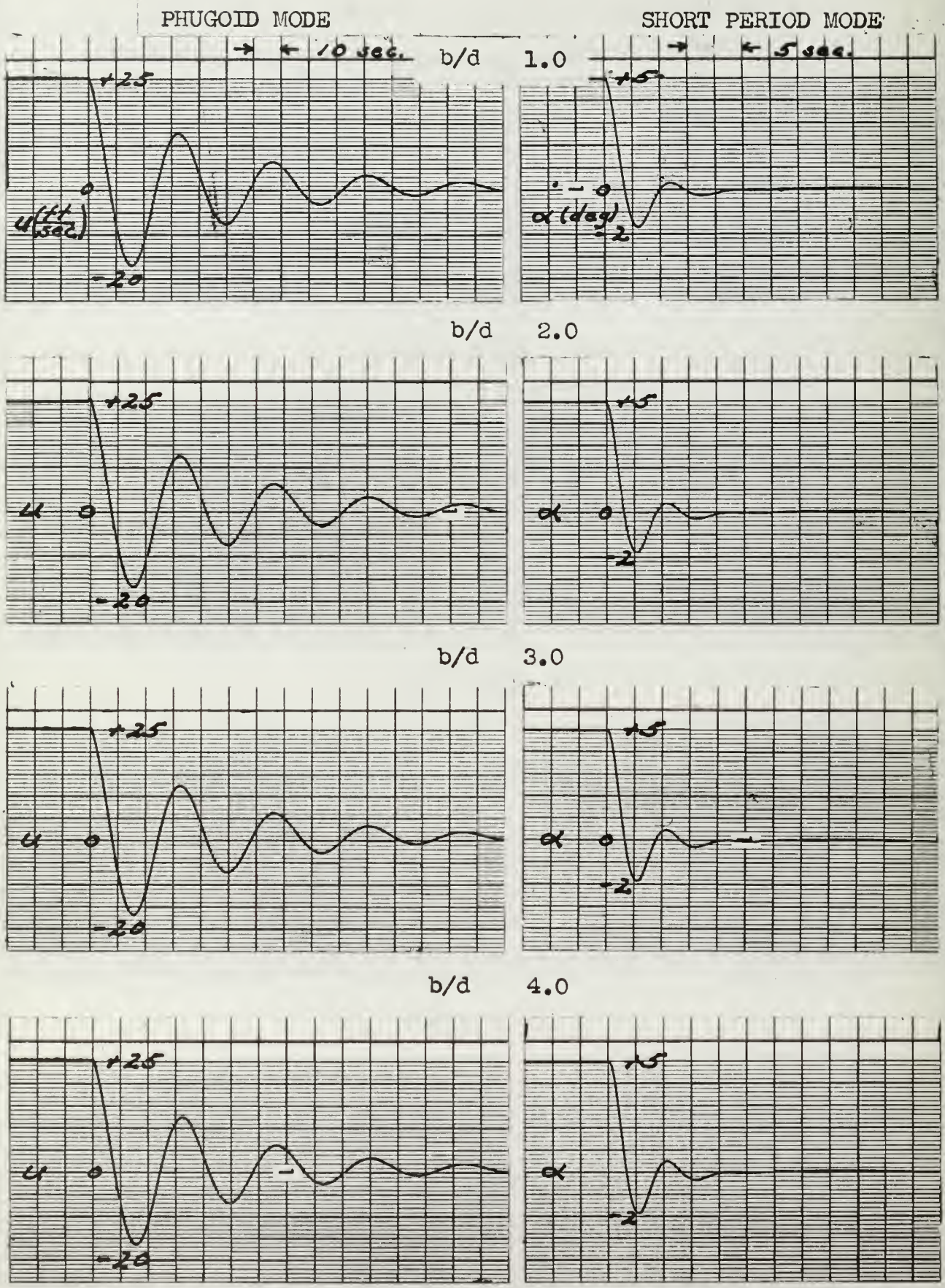

FIGURE 13

ANALOG MECHANIZATION OF

VARIABLE M_α

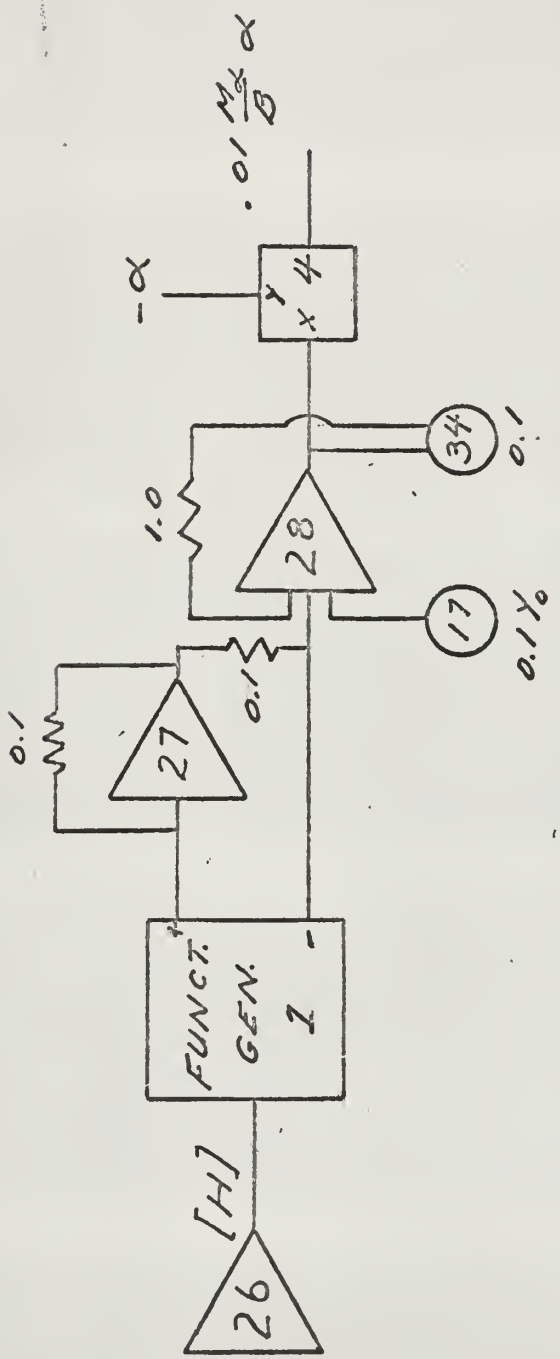

FIGURE 14a

AUTO-THROTTLE FOR u(0) = 5 kt.

WITHOUT GROUND EFFECT

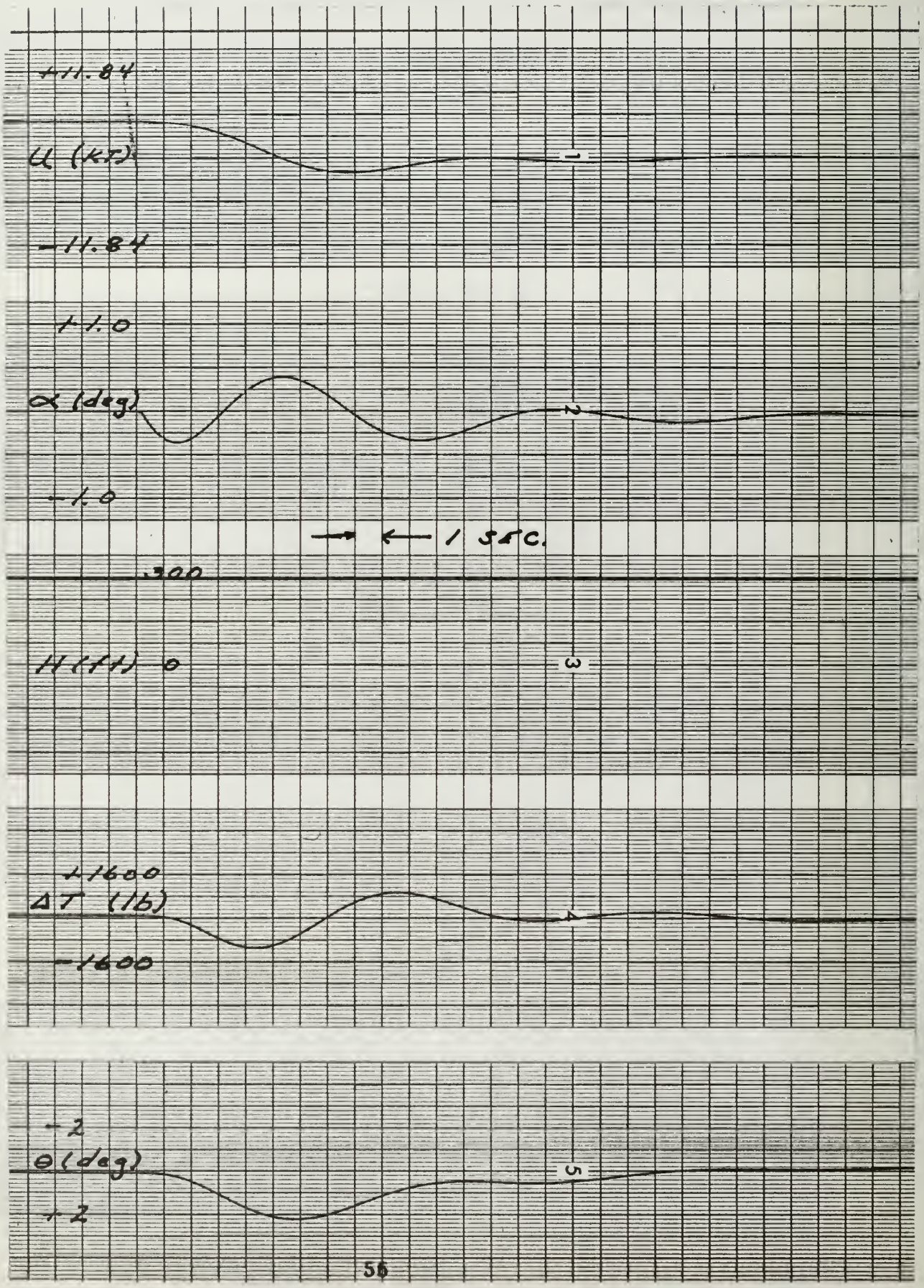

FIGURE 14b

AUTO-THROTTLE FOR u(0) = 5 kt.

WITH GROUND EFFECT

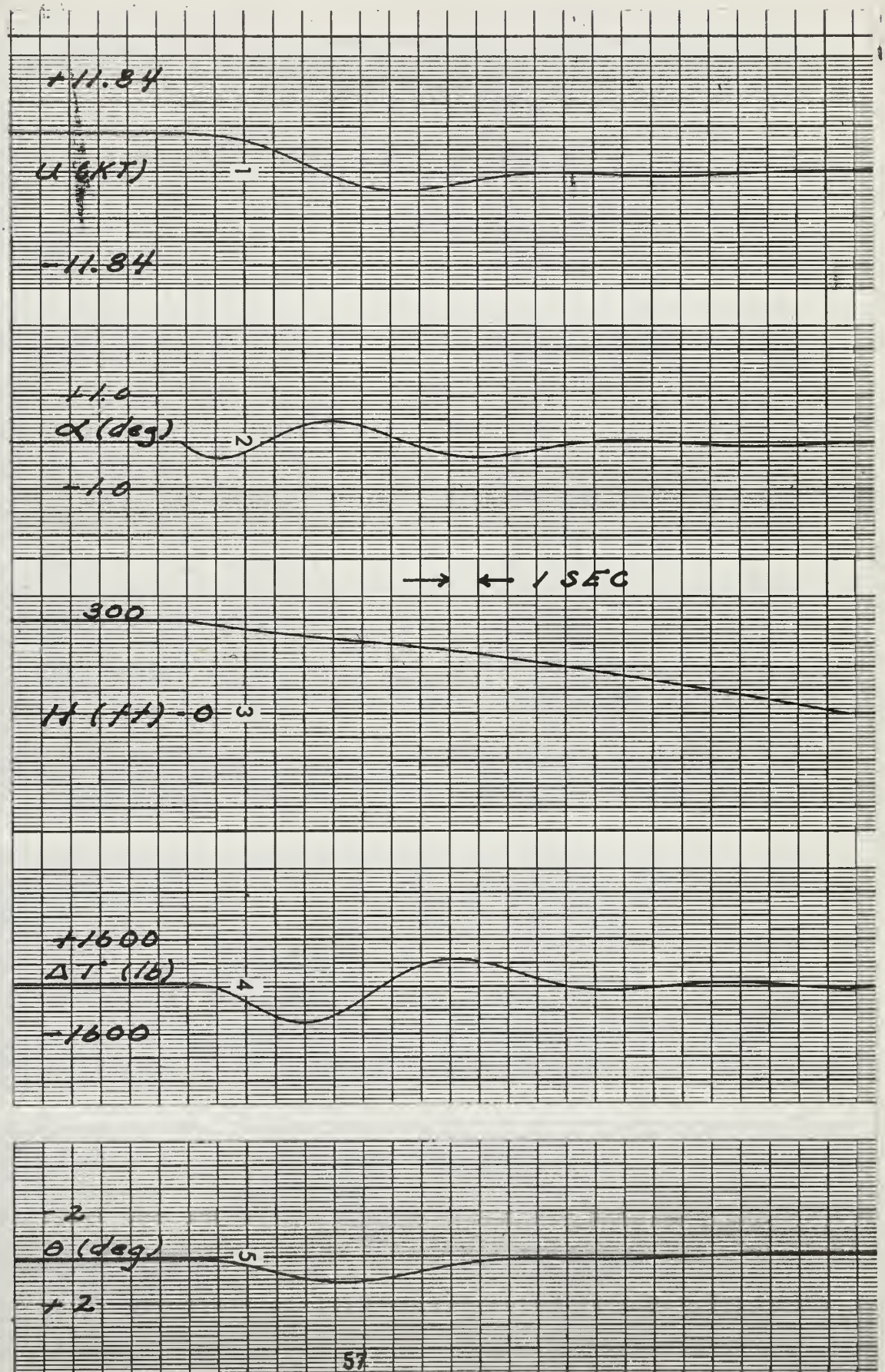

FIGURE 15a

AUTO-THROTTLE FOR $\alpha(0) = 5^{\circ}$

WITHOUT GROUND EFFECT

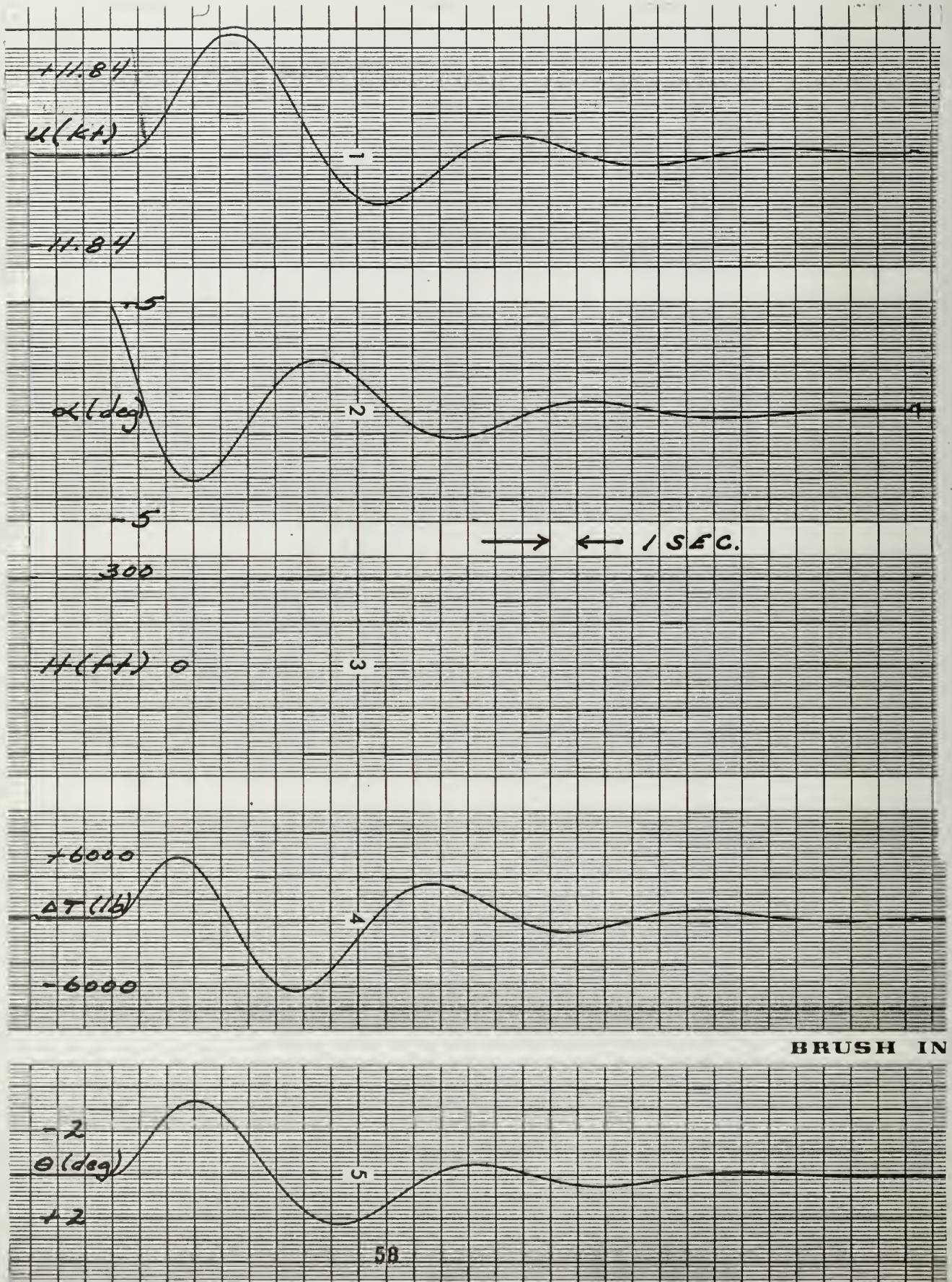

FIGURE 15b

AUTO-THROTTLE FOR $\alpha(0) = .5^{\circ}$

WITH GROUND EFFECT

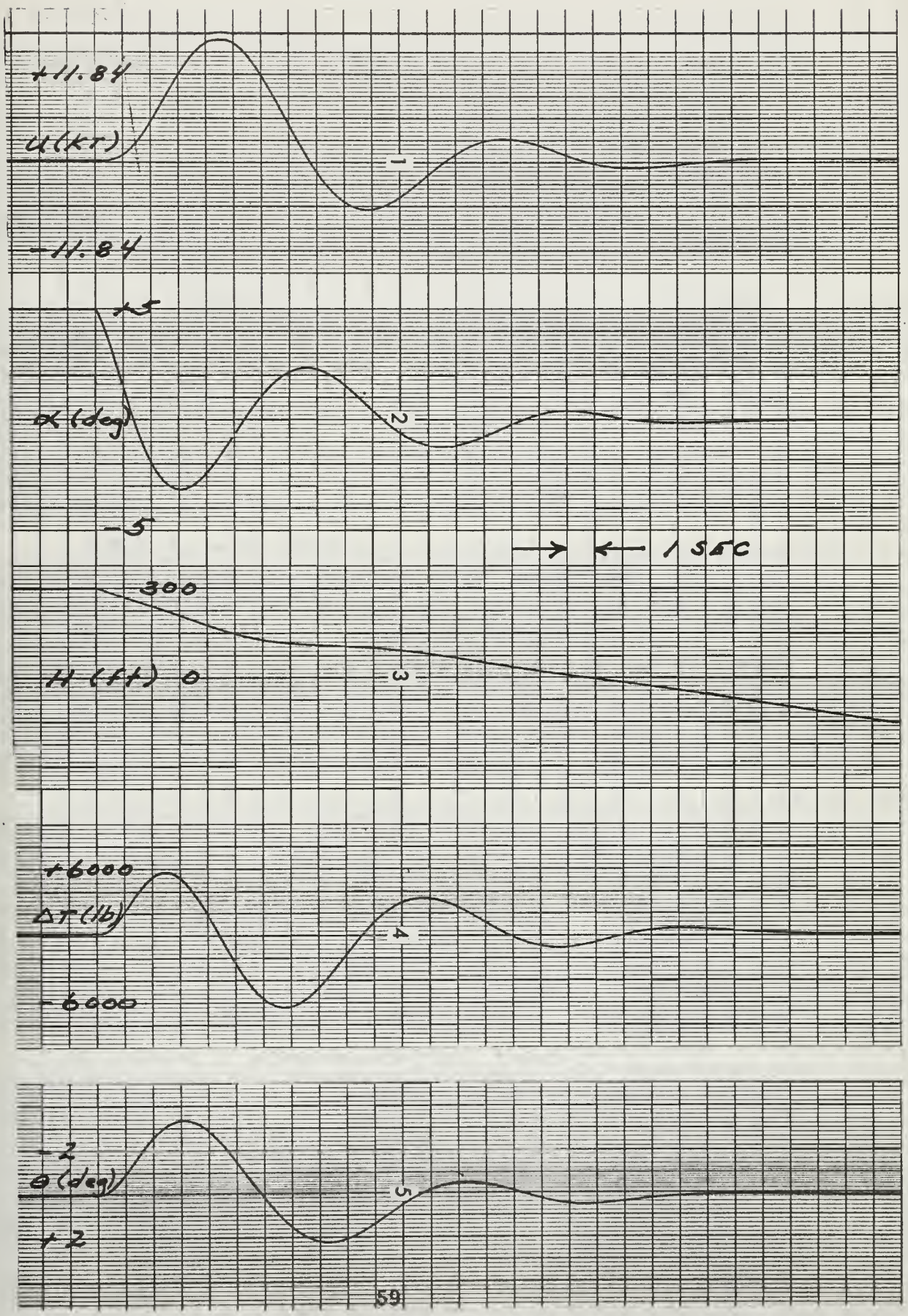

FIGURE 16

AUTO-THROTTLE FOR $\Theta(0) = 4^\circ$

WITHOUT GROUND EFFECT

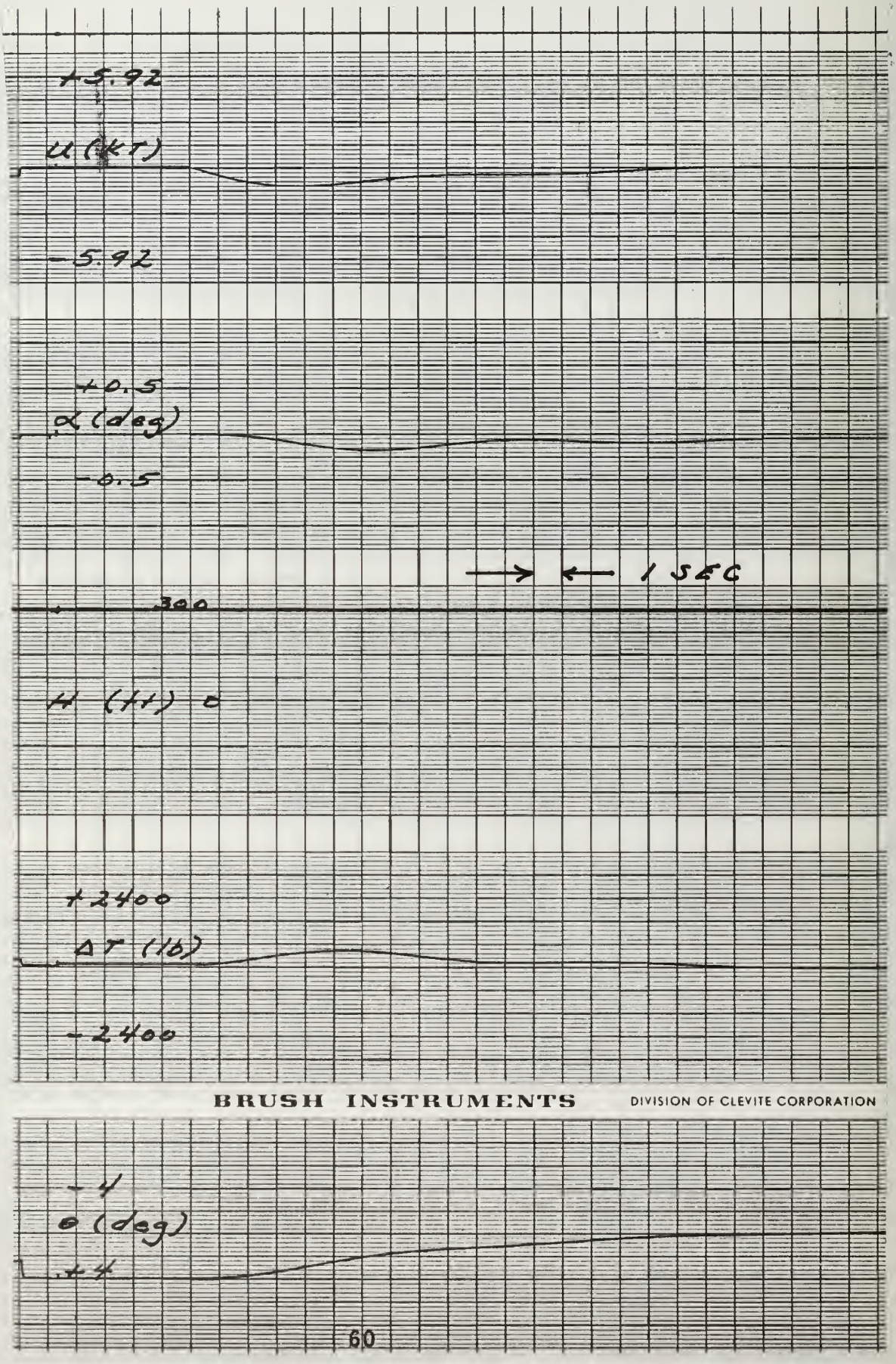

FIGURE 17

RESPONSE DURING FLARE
WITH CONSTANT THRUST

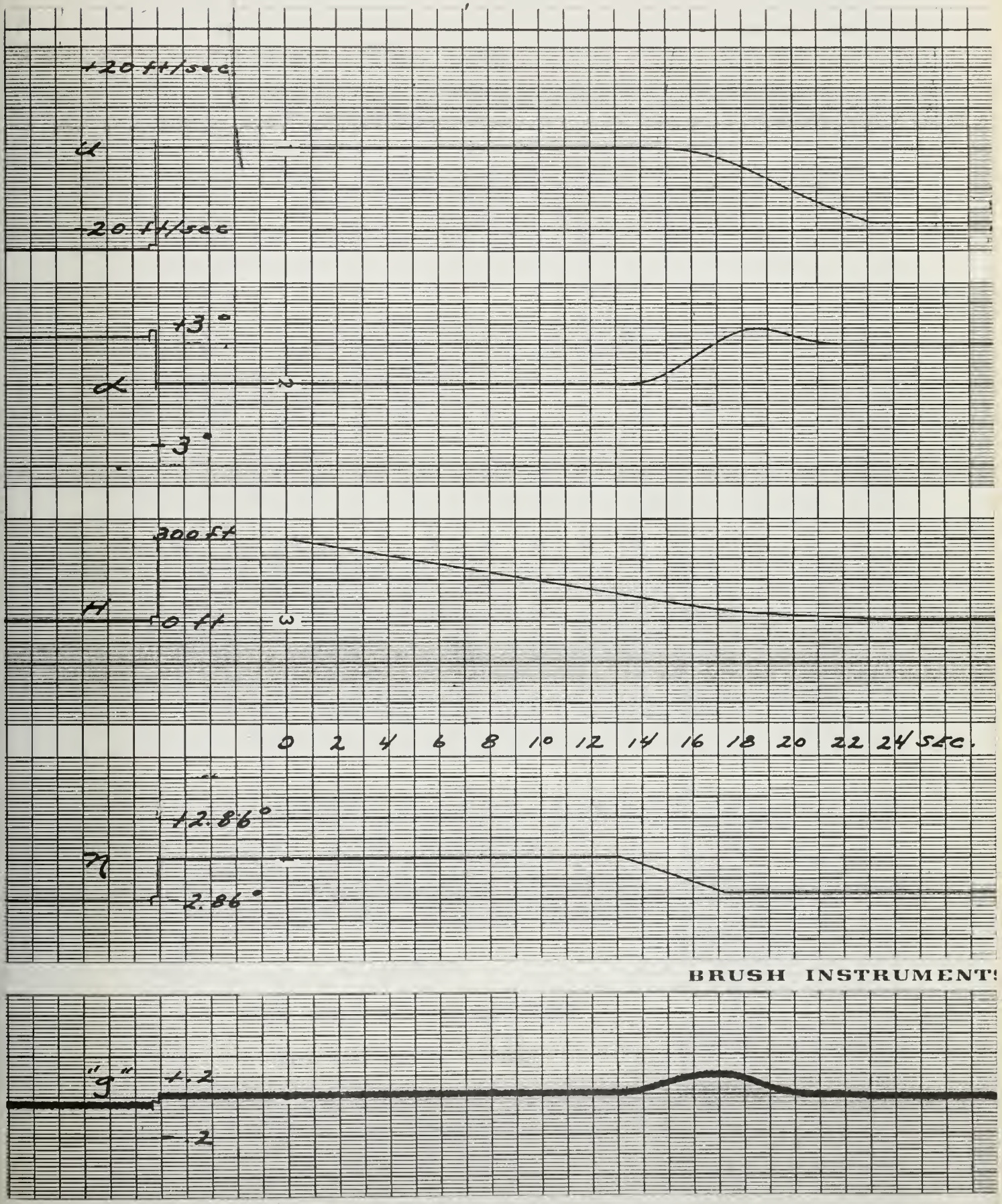

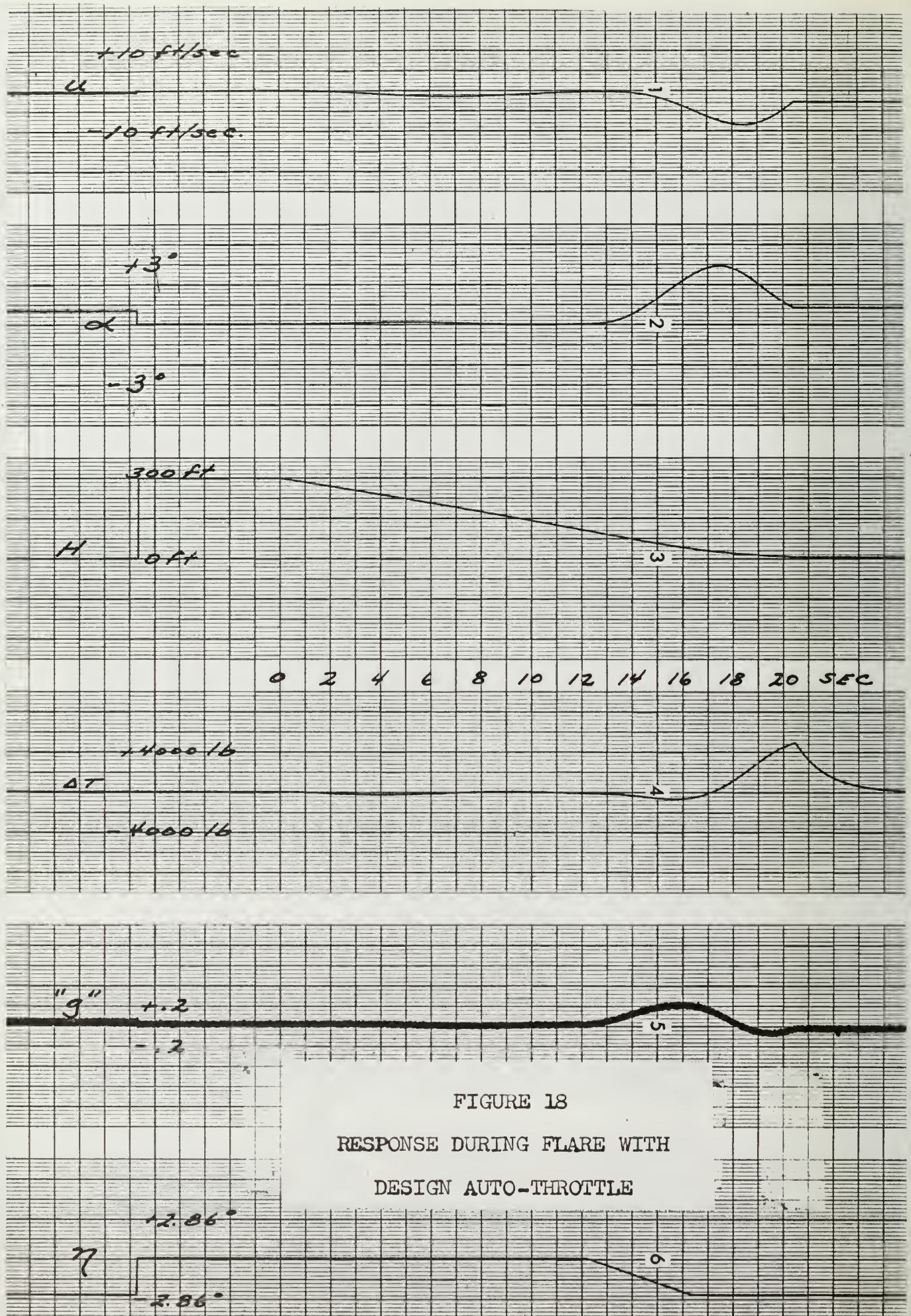

FIGURE 18

RESPONSE DURING FLARE WITH

DESIGN AUTO-THROTTLE

FIGURE 19

ANALOG MECHANIZATION OF

BIAS SYSTEM

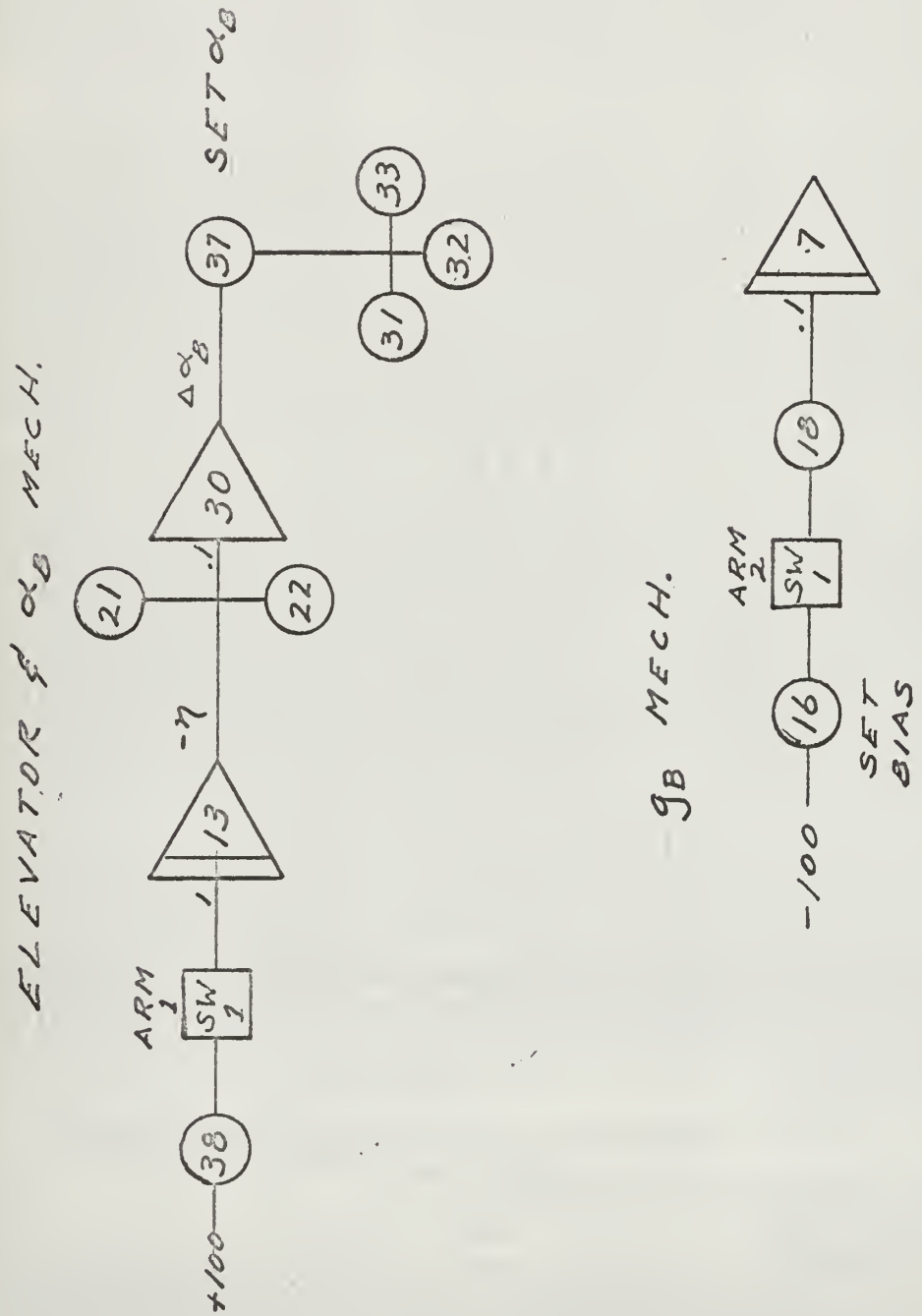

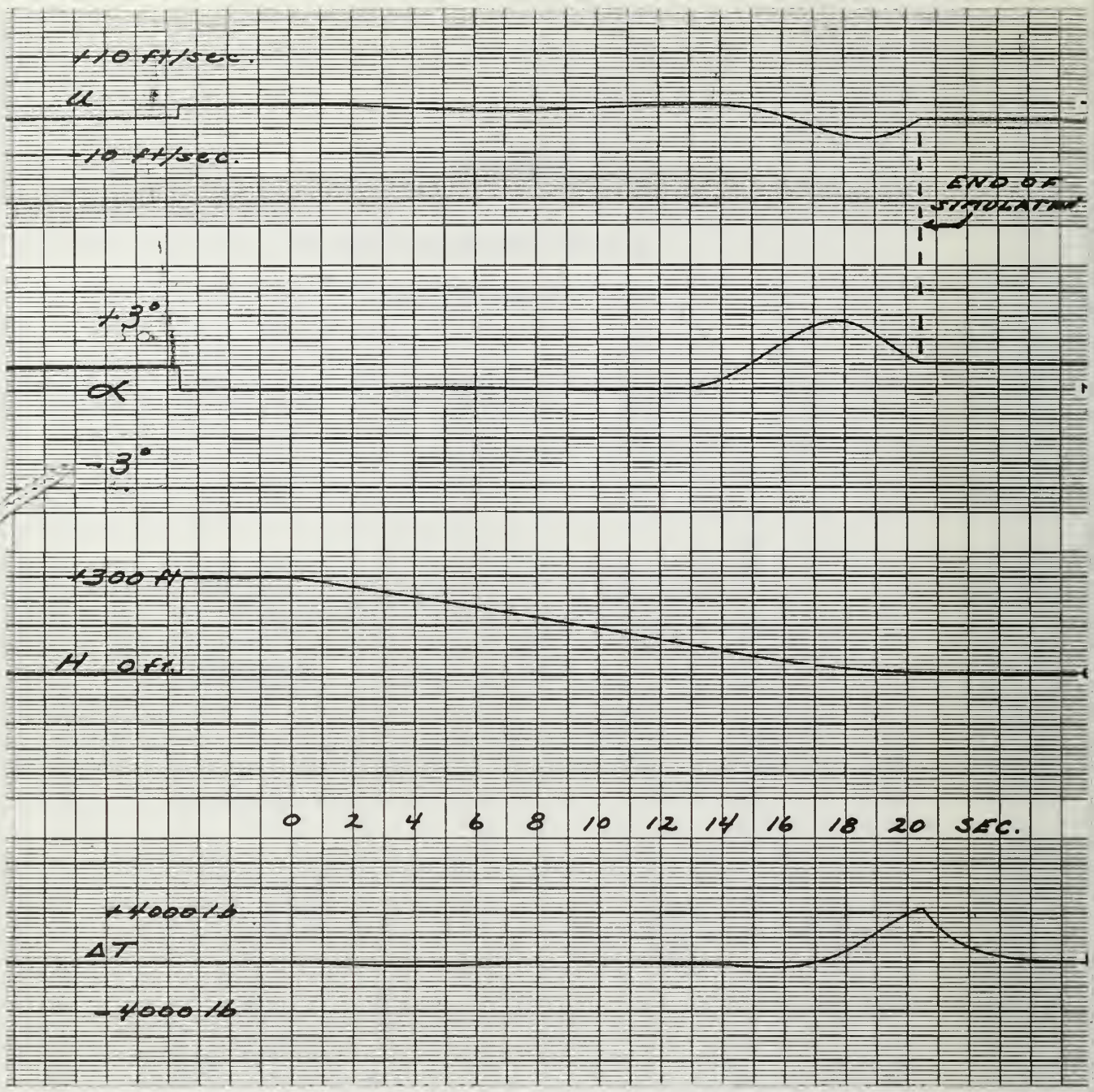

BRUSH INSTRUMENTS DIVISION OF CLEVITE CORPORATION

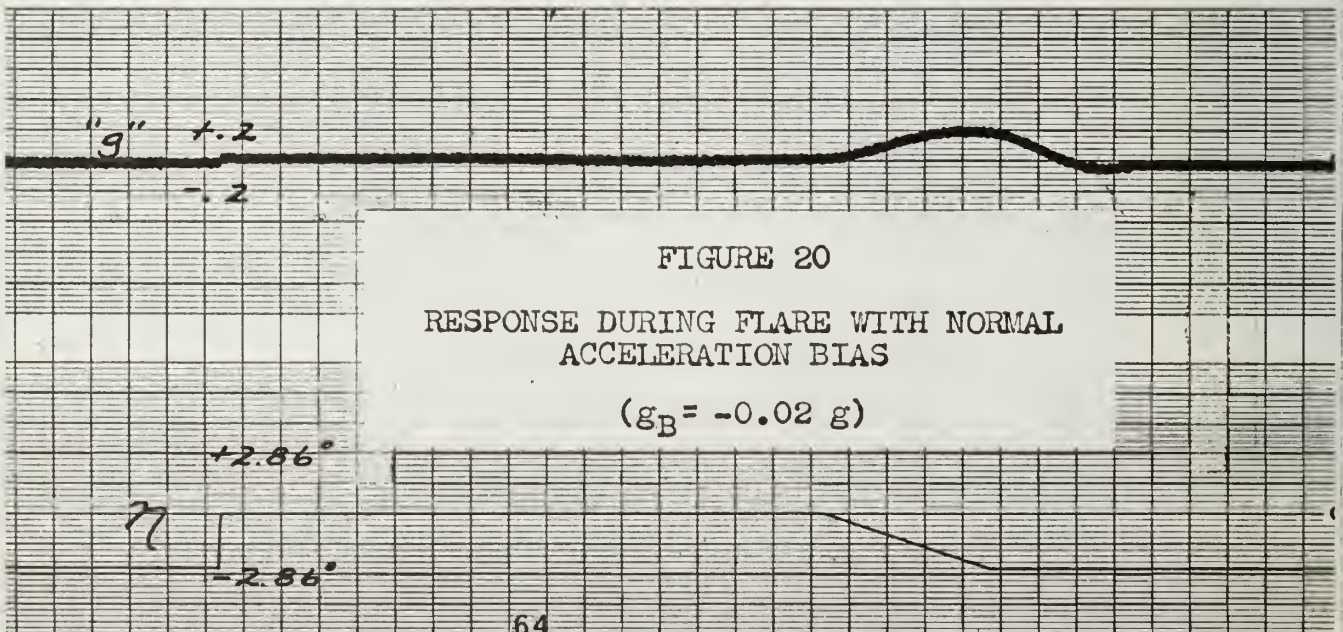

FIGURE 20

RESPONSE DURING FLARE WITH NORMAL ACCELERATION BIAS

(g_B = -0.02 g)

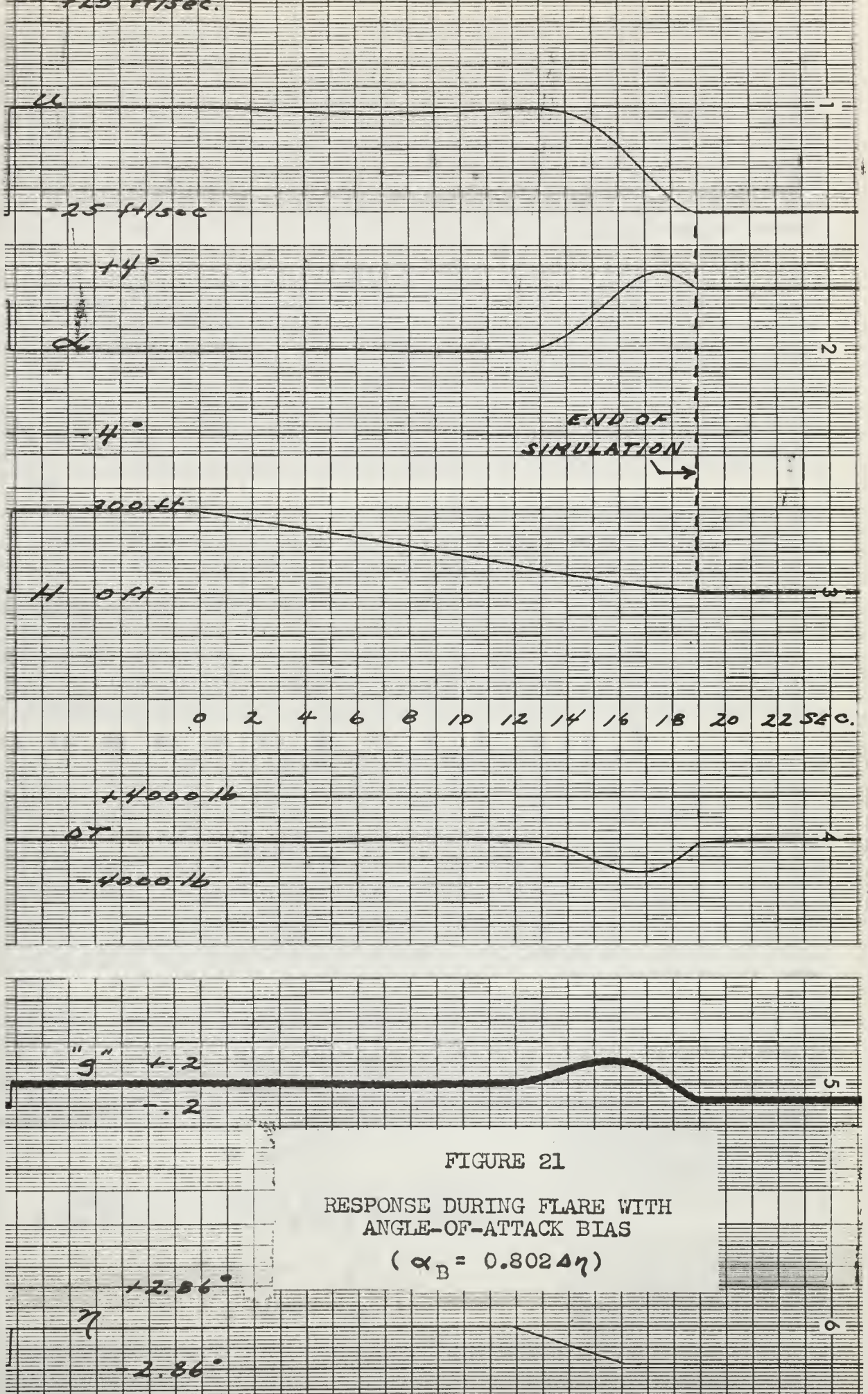

FIGURE 21

RESPONSE DURING FLARE WITH ANGLE-OF-ATTACK BIAS

($\alpha_B = 0.802\Delta\eta$)

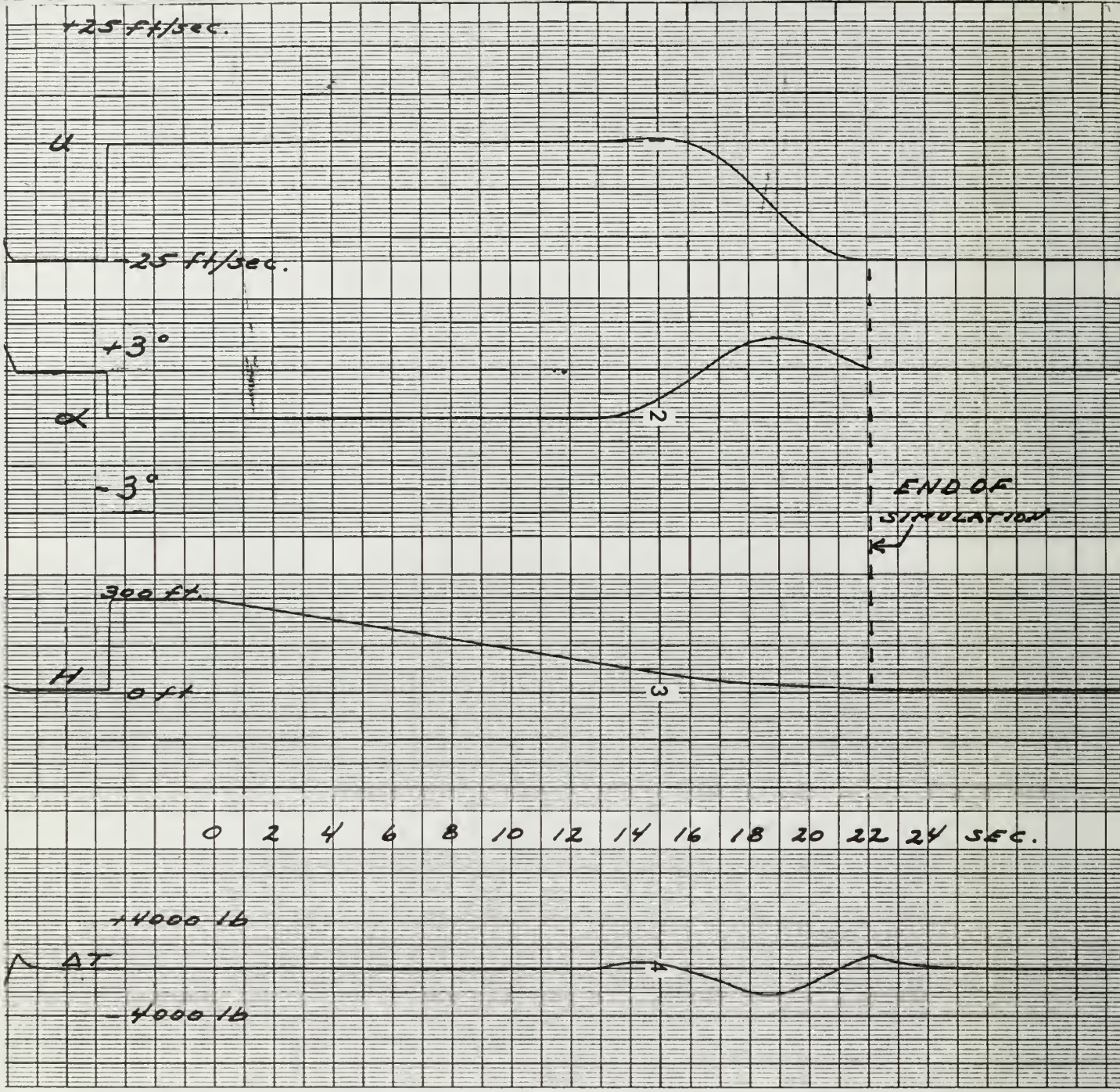

SH INSTRUMENTS DIVISION OF CLEVITE CORPORATION CLEVELAND, OHIO PRINTED IN U.S.A

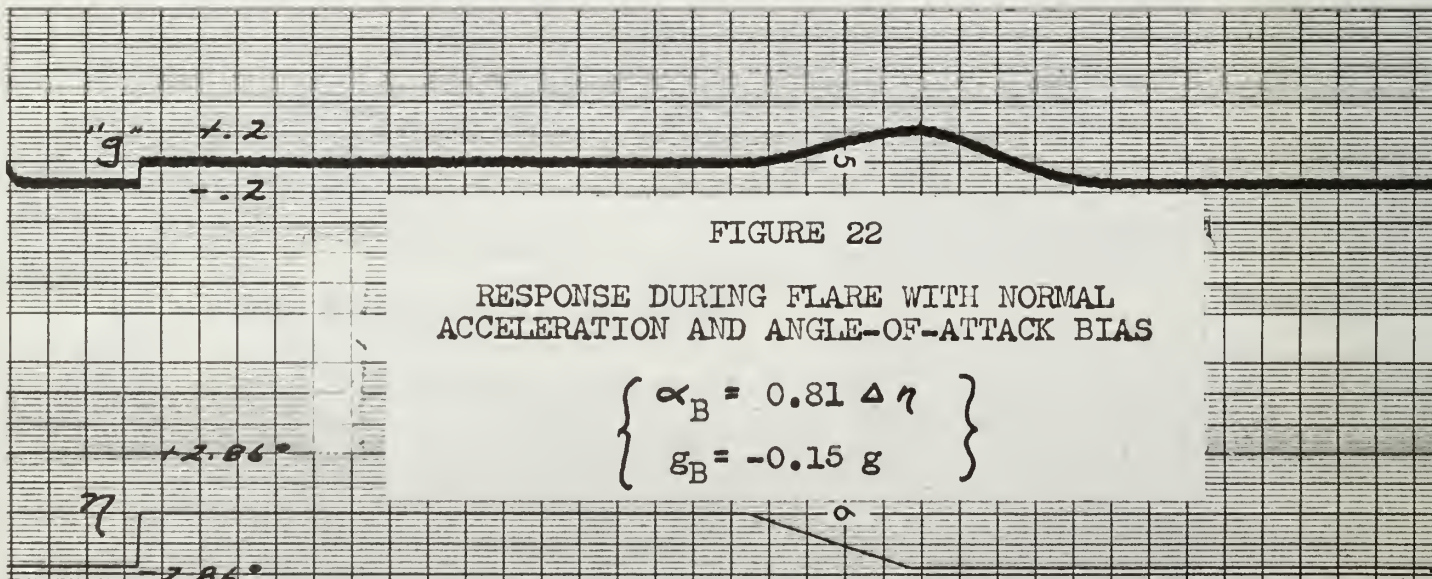

FIGURE 22

RESPONSE DURING FLARE WITH NORMAL ACCELERATION AND ANGLE-OF-ATTACK BIAS

$$\left\{ \begin{array}{l} \alpha_B = 0.81\,\Delta\eta \\ g_B = -0.15\,g \end{array} \right\}$$

APPENDIX I

EQUATIONS OF MOTION

The basic three degrees of freedom aircraft longitudinal equations of motion as derived from small perturbation theory based on body axes are:

X Force:

$$\left[m\frac{\partial}{\partial t} - X_u\right]u - wX_w + \left[mg\cos\Theta - X_q\frac{\partial}{\partial t}\right]\theta = X(t)$$

Z Force:

$$-uZ_u + \left[m\frac{\partial}{\partial t} - Z_w\right]w - \left[(mU_o + Z_q)\frac{\partial}{\partial t}\right]\theta + mg\sin\Theta = Z(t)$$

Moment Equation:

$$-uM_u - wM_w - \dot{w}M_{\dot{w}} + \ddot{\theta}B - \dot{\theta}M_q = M(t)$$

Rearranging, substituting in forcing functions of thrust and elevator, and neglecting minor terms X_q, X_η, Z_q, $\sin\Theta$, and $Z_{\Delta T}$ the equations become:

X Force:

$$\dot{u} - \frac{X_u}{m}u - \frac{X_\alpha}{m}\alpha + g\cos\Theta\theta = \frac{X_{\Delta T}}{m}\Delta T$$

where $$\alpha = \frac{w}{U_o}$$

Z Force:

$$-\frac{1}{mU_o}Z_u u + \dot{\alpha} - \frac{Z_w}{m}\alpha - \dot{\theta} = \frac{Z_\eta}{mU_o}\eta$$

Moment Equation:

$$-\frac{M_u}{B}u - \frac{M_{\dot{\alpha}}}{B}\dot{\alpha} - \frac{M_\alpha}{B}\alpha + \ddot{\theta} - \frac{M_q}{B}\dot{\theta} = \frac{M_{\Delta T}}{B}\Delta T + \frac{M_\eta}{B}\eta$$

Figure defining signs:

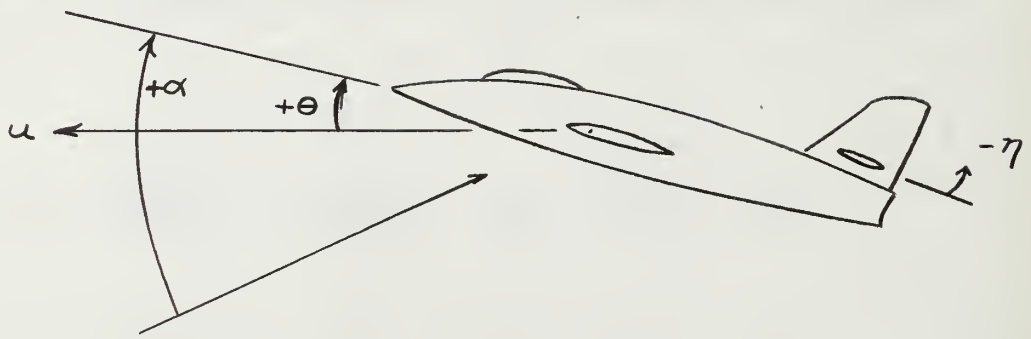

Definitions of Stability Derivatives:

$$X_u = -\rho U_o S_w (C_D + C_{D_u})$$

$$X_w = \tfrac{1}{2}\rho U_o S_w (C_L - C_D)$$

$$X_\alpha = U_o X_w$$

$$X_{\Delta T} = \cos(\alpha_o + \zeta)$$

$$Z_u = -\rho U_o S_w (C_L + C_{L_u})$$

$$Z_w = -\tfrac{1}{2}\rho U_o S_w (C_{L\alpha} + C_D)$$

$$Z_\eta = -\tfrac{1}{2}\rho U_o^2 S_w C_{L\eta}$$

$$M_u = \rho U_o S_w \bar{c} (C_m + \tfrac{1}{2} U_o C_{m_u})$$

$$M_{\dot{\alpha}} = U_o (-\tfrac{1}{2} S_T l_T^2 C_{L\alpha T} \frac{d\epsilon}{d\alpha})$$

$$M_\alpha = U_o M_w = U_o (\tfrac{1}{2}\rho U_o S \bar{c} C_{m_\alpha})$$

$$Mq = \tfrac{1}{4}\bar{c}\rho U_o S_w \bar{c} C_{mq})$$

$$M_{\Delta T} \cong -0.437$$

$$M_\eta = \tfrac{1}{2}\rho U_o^2 S \bar{c} C_{m_\eta})$$

Substituting the values given in Table I:

X Force:

$$\dot{u} + .0602\,u + 3.325\,\alpha + 31.88\,\theta = .00145\,\Delta T$$

Z Force:

$$.00113\,u + \dot{\alpha} + .4271\,\alpha - \dot{\theta} = -.0595\,\eta$$

Moment Equation:

$$-1.89 \times 10^{-4}\,u + .041\,\dot{\alpha} + 1.139\,\alpha + \ddot{\theta} + .3396\,\dot{\theta}$$
$$= -.455 \times 10^{-5}\,\Delta T - 2.504\,\eta$$

APPENDIX II

STABILITY DERIVATIVES FOR GROUND EFFECT

X_α:

$$X_\alpha = \tfrac{1}{2}\rho U_o^2 S_W C_L \left(1 - \frac{2\,C_{L\alpha}}{e\pi A}\right)$$

$$= \tfrac{1}{2}\rho U_o^2 S_W C_L \left[1 - \frac{2}{e\pi A} C_{L\alpha} \frac{(C_{L\alpha})_G}{(C_{L\alpha})}\right]$$

Z_w:

$$Z_w = -\tfrac{1}{2}\rho U_o S_W \left(C_{L\alpha} + C_D\right)$$

$$= -\tfrac{1}{2}\rho U_o S_W \left[C_{L\alpha} \frac{(C_{L\alpha})_G}{(C_{L\alpha})} + C_D\right]$$

M_α:

$$M_\alpha = U_o M_w = U_o \left[\tfrac{1}{2}\rho U_o S_W \bar{c}\, C_{m\alpha}\right]$$

$$C_{m\alpha} = C_{L\alpha_{wb}} \left(h - h_{n_{wb}}\right) - V_H C_{L\alpha_T} \left(1 - \frac{\partial \epsilon}{\partial \alpha}\right)$$

$$= C_{L\alpha_{wb}} \frac{(C_{L\alpha_{wb}})_G}{(C_{L\alpha_{wb}})} \left(h - h_{n_{wb}}\right)$$

$$- V_H C_{L\alpha_T} \frac{(C_{L\alpha_T})_G}{(C_{L\alpha_T})} \left[1 - \left(\frac{\partial \epsilon}{\partial C_L}\right)\left(\frac{\partial C_L}{\partial \alpha}\right) \frac{\left(\frac{\partial \epsilon}{\partial C_L}\right)_G}{\left(\frac{\partial \epsilon}{\partial C_L}\right)} \frac{\left(\frac{\partial C_L}{\partial \alpha}\right)_G}{\left(\frac{\partial C_L}{\partial \alpha}\right)}\right]$$

$M_{\dot\alpha}$:

$$M_{\dot\alpha} = U_o M_{\dot w} = \tfrac{1}{2}\rho S_T \ell_T^2 C_{L\alpha_T} \frac{\partial \epsilon}{\partial \alpha}$$

$$M_{\dot{\alpha}} = -\frac{1}{2}\rho S_T \ell_T^2 C_{L\alpha_T} \frac{(C_{L\alpha_T})_G \left(\frac{\partial \epsilon}{\partial C_L}\right)\left(\frac{\partial \epsilon}{\partial C_L}\right)_G (C_{L\alpha})(C_{L\alpha})_G}{(C_{L\alpha_T})\left(\frac{\partial \epsilon}{\partial C_L}\right)(C_{L\alpha})}$$

$$= -3940.41 \left[\frac{(C_{L\alpha})_G}{(C_{L\alpha})} \frac{\left(\frac{\partial \epsilon}{\partial C_L}\right)_G}{\left(\frac{\partial \epsilon}{\partial C_L}\right)} \frac{(C_{L\alpha})_G}{(C_{L\alpha})}\right]$$

APPENDIX III

ANALOG FORM OF AUTO-THROTTLE EQUATIONS

$$\Delta T = \frac{1}{(1+\tau_e S)} \frac{1}{(1+\tau_S S)} \left[\left(\frac{K\alpha}{1+\tau_\alpha S} + \frac{K\dot{\alpha}}{S} + \frac{K\int}{1+S} \right) \alpha - \frac{Kn}{1+\tau_n S} n \right]$$

$$= \frac{1}{(1+1.2S)} \frac{1}{(1+.2S)} \left[\left(\frac{570}{1+.5S} + \frac{190}{S} + \frac{1100}{1+S} \right) \alpha - \frac{19,400}{1+S} n \right]$$

Equation without time elements

$$\Delta T = 570(57.3)\alpha + 190(57.3)\int\alpha + (1100)(57.3)\alpha - 19,400n$$

$$a_{\Delta T}\Delta\bar{T} = 32,661 a_\alpha \bar{\alpha} + 10,887\, a_{\int\alpha} \int\bar{\alpha} + 63,000\, a_\alpha \bar{\alpha} - 19,400\, a_n \bar{n}$$

$$\Delta\bar{T} = .71\,\bar{\alpha} + .237\int\bar{\alpha} + 1.371\,\bar{\alpha} - 4.85\,\bar{n}$$

where:

K_α = 570 lb./deg. = 32,661 lb./rad.

K_γ = 190 lb./deg-sec. = 10,887 lb./rad-sec.

$K_{,}$ = 11,000 lb./deg. = 63,000 lb./rad.

K_n = 19,400 lb./g

APPENDIX IV

ANALOG DERIVATION OF AUXILIARY EQUATIONS

Acceleration:

$$n = \ddot{h} \text{ (normal to flt. path)} = V_{Total}\,\dot{\gamma}$$

$$= (U_o + u)\,\frac{d}{dt}(\theta - \alpha)$$

$$= (U_o + u)\,(\dot{\theta} - \dot{\alpha})$$

$$a_n \bar{n} = (a_{U_o} \bar{U}_o + a_u \bar{u})\,(a_{\dot{\theta}} \dot{\bar{\theta}} - a_{\dot{\alpha}} \dot{\bar{\alpha}})$$

$$.02\,\bar{n} = (3.0\,\bar{U}_o + .5\,\bar{u})\,(.00349\,\dot{\bar{\theta}} - .001745\,\dot{\bar{\alpha}})$$

$$\frac{n}{g}(\text{"g" units}) = \frac{3.11}{100}(\bar{U}_o + .167\,\bar{u})\,(.524\,\dot{\bar{\theta}} - .262\,\dot{\bar{\alpha}})$$

Glide Slope:

From Appendix I; $\gamma = \theta - \alpha$

$$a_\gamma \bar{\gamma} = a_\theta \bar{\theta} - a_\alpha \bar{\alpha}$$

$$.00349\,\bar{\gamma} = .00349\,\bar{\theta} - .001745\,\bar{\alpha}$$

$$\bar{\gamma} = \bar{\theta} - .5\,\bar{\alpha}$$

Total Altitude:

H_o - Initial altitude = 300 ft.

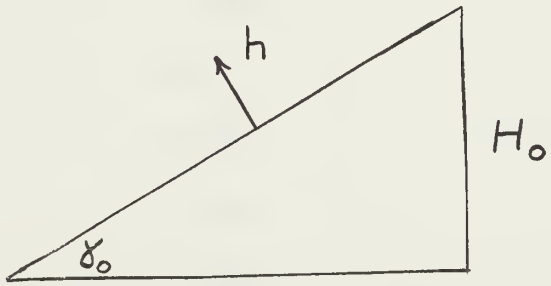

$$H = H_o - U_o(t) \sin \gamma_o + h$$

$$= H_o - \gamma_o (\text{rad}) \int U_o + \iint \ddot{h}$$

$$= H_o - \gamma_o \int U_o + \iint V_T \dot{\gamma}$$

$$= H_o - .07 \int U_o + (U_o + u) \int \gamma$$

$$a_H \bar{H} = a_{H_o} \bar{H}_o - .07 \int a_{U_o} \bar{U}_o + (a_{U_o} \bar{U}_o + a_u \bar{u}) \int a_\gamma \bar{\gamma}$$

$$3.0\bar{H} = 3.0\bar{H}_o - .07 \int 3.0\bar{U}_o + (3.0\bar{U}_o + .5\bar{u}) \int .00349\, \bar{\gamma}$$

$$\bar{H} = \bar{H}_o - .07 \int \bar{U}_o + (\bar{U}_o + .167\, \bar{u})(.0087) \int \frac{\bar{\gamma}}{2.5}$$

APPENDIX V

ANALOG POTENTIOMETER SETTINGS

Potentiometer	Coefficient of (Equat.)	Setting
1	$u\ (\dot{u})$	.0602
2	$\theta\ (\dot{u})$	.2252
3	$\alpha\ (\dot{u})$	.0116
4	$\alpha\ (\dot{\alpha})$	.4271
5	$u\ (\dot{\alpha})$	.3238
6	$u\ (\ddot{\theta})$	.0271
7	$\dot{\alpha}\ (\ddot{\theta})$	.0205
8	$\dot{\theta}\ (\ddot{\theta})$	.3396
9	$\alpha\ (\gamma)$	.5
10	$V_T(h)$	.87
11	$\gamma\ (h)$	.5
12	$\alpha\ (K_1 - T)$	.1371
13	$n\ (K_n - T)$	.485
14	$\alpha\ (K_\gamma - T)$	.237
15	$\alpha\ (K_\alpha - T)$	.71
16	g_B	variable
17	$Y_o\ (h)$	.093
21	$\eta\ (\theta)$	.358
22	$\eta\ (\dot{\alpha})$	.1705
23	$U_o\ (V_T)$	.78

Potentiometer	Coefficient of (Equat.)	Setting
24	$u\ (V_T)$	.167
25	$U_o\ (\delta \int U_o)$	.0275
26	$H_o\ (H)$	1.0
28	$\dot{\theta}\ (\Delta n)$	.524
29	$\dot{\alpha}\ (\Delta n)$	.262
30	$g\ (\Delta n)$	.311
31	$\alpha_B\ (K_1 - T)$	.1371
32	$\alpha_B\ (K_\delta - T)$	.237
33	$\alpha_B\ (K_\alpha - T)$	.71
34	Funct. Gen.	.1
35	$\Delta T\ (\dot{u})$	.232
36	$\Delta T\ (\ddot{\theta})$	.1043
37	α_B	variable
38	η	variable

INITIAL DISTRIBUTION LIST

		No. Copies
1.	Defense Documentation Center Cameron Station Alexandria, Virginia 22314	20
2.	Library U. S. Naval Postgraduate School Monterey, California	2
3.	Commander, Naval Air Systems Command Department of the Navy Washington, D.C. 20360	1
4.	Chairman, Department of Aeronautics U.S. Naval Postgraduate School Monterey, California	2
5.	Prof E. J. Andrews Department of Aeronautics U.S. Naval Postgraduate School Monterey, California	1
6.	LCDR Robert Louis Elich, USN 2502 Columbine Pueblo, Colorado	1

DOCUMENT CONTROL DATA - R&D

(Security classification of title, body of abstract and indexing annotation must be entered when the overall report is classified)

1. ORIGINATING ACTIVITY *(Corporate author)* U.S. Naval Postgraduate School Monterey, California	2a. REPORT SECURITY CLASSIFICATION UNCLASSIFIED 2b. GROUP

3. REPORT TITLE

AN AUTOMATIC-THROTTLE DEVICE FOR AIRSPEED CONTROL DURING FLARE TO FIELD LANDINGS

4. DESCRIPTIVE NOTES *(Type of report and inclusive dates)*

Thesis - M.S. Aero

5. AUTHOR(S) *(Last name, first name, initial)*

ELICH, Robert L., LCDR, USN

6. REPORT DATE	7a. TOTAL NO. OF PAGES	7b. NO. OF REFS
May 1966	76	5

8a. CONTRACT OR GRANT NO.	9a. ORIGINATOR'S REPORT NUMBER(S)
b. PROJECT NO.	NONE
c.	9b. OTHER REPORT NO(S) *(Any other numbers that may be assigned this report)*
d.	NONE

10. AVAILABILITY/LIMITATION NOTICES

Qualified requesters may obtain copies of this report from DDC.

11. SUPPLEMENTARY NOTES	12. SPONSORING MILITARY ACTIVITY
	Naval Air Systems Command Navy Department, Washington, D.C.

13. ABSTRACT

This study is a continuation of the investigations in the use of automatic-throttle compensation systems. The previous investigations demonstrated the capability of such systems in alleviating the problems of aircraft speed instability in the carrier landing approach. The feasibility of adapting the system with sensed-input variables of angle-of-attack and normal acceleration to the condition of field landings with flare was investigated. An analysis of the ground effect prevalent in field landings was performed and the significant influences on aircraft response were included in the investigation. The desired airspeed control with zero rate of descent at touchdown was obtained by incorporating additional commands in the basic auto-throttle device during the flare maneuver. The analog computer was utilized for problem simulation.

DD FORM 1 JAN 64 1473

14. KEY WORDS	LINK A		LINK B		LINK C	
	ROLE	WT	ROLE	WT	ROLE	WT
Automatic-Throttle Flare Landings Power Compensator						

INSTRUCTIONS

1. ORIGINATING ACTIVITY: Enter the name and address of the contractor, subcontractor, grantee, Department of Defense activity or other organization *(corporate author)* issuing the report.

2*a*. REPORT SECURITY CLASSIFICATION: Enter the overall security classification of the report. Indicate whether "Restricted Data" is included. Marking is to be in accordance with appropriate security regulations.

2*b*. GROUP: Automatic downgrading is specified in DoD Directive 5200.10 and Armed Forces Industrial Manual. Enter the group number. Also, when applicable, show that optional markings have been used for Group 3 and Group 4 as authorized.

3. REPORT TITLE: Enter the complete report title in all capital letters. Titles in all cases should be unclassified. If a meaningful title cannot be selected without classification, show title classification in all capitals in parenthesis immediately following the title.

4. DESCRIPTIVE NOTES: If appropriate, enter the type of report, e.g., interim, progress, summary, annual, or final. Give the inclusive dates when a specific reporting period is covered.

5. AUTHOR(S): Enter the name(s) of author(s) as shown on or in the report. Enter last name, first name, middle initial. If military, show rank and branch of service. The name of the principal author is an absolute minimum requirement.

6. REPORT DATE: Enter the date of the report as day, month, year, or month, year. If more than one date appears on the report, use date of publication.

7*a*. TOTAL NUMBER OF PAGES: The total page count should follow normal pagination procedures, i.e., enter the number of pages containing information.

7*b*. NUMBER OF REFERENCES: Enter the total number of references cited in the report.

8*a*. CONTRACT OR GRANT NUMBER: If appropriate, enter the applicable number of the contract or grant under which the report was written.

8*b*, 8*c*, & 8*d*. PROJECT NUMBER: Enter the appropriate military department identification, such as project number, subproject number, system numbers, task number, etc.

9*a*. ORIGINATOR'S REPORT NUMBER(S): Enter the official report number by which the document will be identified and controlled by the originating activity. This number must be unique to this report.

9*b*. OTHER REPORT NUMBER(S): If the report has been assigned any other report numbers *(either by the originator or by the sponsor)*, also enter this number(s).

10. AVAILABILITY/LIMITATION NOTICES: Enter any limitations on further dissemination of the report, other than those imposed by security classification, using standard statements such as:

(1) "Qualified requesters may obtain copies of this report from DDC."

(2) "Foreign announcement and dissemination of this report by DDC is not authorized."

(3) "U. S. Government agencies may obtain copies of this report directly from DDC. Other qualified DDC users shall request through _____."

(4) "U. S. military agencies may obtain copies of this report directly from DDC. Other qualified users shall request through _____."

(5) "All distribution of this report is controlled. Qualified DDC users shall request through _____."

If the report has been furnished to the Office of Technical Services, Department of Commerce, for sale to the public, indicate this fact and enter the price, if known.

11. SUPPLEMENTARY NOTES: Use for additional explanatory notes.

12. SPONSORING MILITARY ACTIVITY: Enter the name of the departmental project office or laboratory sponsoring *(paying for)* the research and development. Include address.

13. ABSTRACT: Enter an abstract giving a brief and factual summary of the document indicative of the report, even though it may also appear elsewhere in the body of the technical report. If additional space is required, a continuation sheet shall be attached.

It is highly desirable that the abstract of classified reports be unclassified. Each paragraph of the abstract shall end with an indication of the military security classification of the information in the paragraph, represented as *(TS)*, *(S)*, *(C)*, *or (U)*.

There is no limitation on the length of the abstract. However, the suggested length is from 150 to 225 words.

14. KEY WORDS: Key words are technically meaningful terms or short phrases that characterize a report and may be used as index entries for cataloging the report. Key words must be selected so that no security classification is required. Identifiers, such as equipment model designation, trade name, military project code name, geographic location, may be used as key words but will be followed by an indication of technical context. The assignment of links, roles, and weights is optional.

DD FORM 1 JAN 64 1473 (BACK)